A new wave in fluid dynamics

Propagation of simultaneous operational and geometrical uncertainties in an integrated CFD design environment by means of a sparse collocation method

Remy Nigro*, Dirk Wunsch**, Gregory Coussement*, Charles Hirsch**
*University of Mons, **Numeca International

Dresden, 08.10.2014

Outline

- **Context**
- UQ tool for simultaneous operational and geometrical uncertainties implemented in FINE™
- Application of Uncertainty Quantification in Industrial Applications
- Perspective

The role of uncertainties in Virtual Prototyping

Paradigm shift in Virtual Prototyping (VP) methodology

- Virtual Prototyping (VP) has become the key technology for industry
  - Reduce product development cycle costs
  - Respond to the challenges of designing sustainable products and responding to the environmental challenges
- These objectives require a highly integrated computer-based design system,
  - Relying on advanced massively parallel hardware, making the virtual product development and qualification process more realizable
- Example: 3-D viscous flow analysis of engine components uncertainties:
  - In the boundary conditions representing the operational environment;
  - On the geometry resulting from manufacturing tolerances and assembly process.
  - In modeling uncertainties and numerical errors (such as grid dependences)
- These uncertainties lead to a global uncertainty on the results of the analysis
  - Which is used as the basis for design decisions!

The role of uncertainties in Virtual Prototyping

Paradigm shift in Virtual Prototyping (VP) methodology

- Predicted quantities, such as loads, lift, drag, efficiencies, temperatures, ….
  - Now represented by a Probability Density Function (PDF)
  - This PDF provides a domain of confidence associated to the considered uncertainties

- This corresponds to a fundamental shift in paradigm for the whole of the VP methodology

Result of deterministic CFD simulations for mean value of measured uncertainty parameter as input

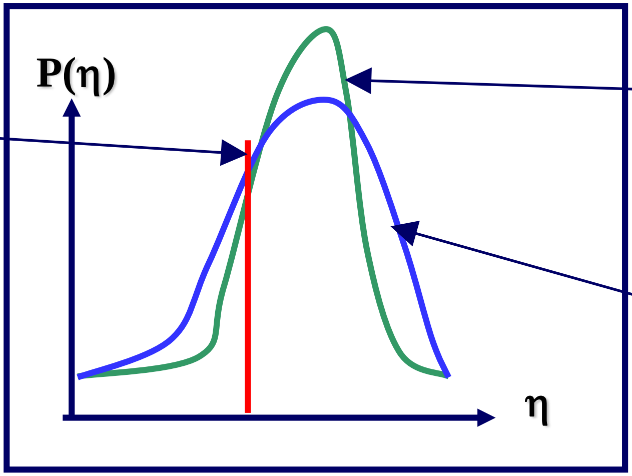

PDF of non-deterministic CFD simulations for <u>given PDF of uncertainty parameter as input</u>

PDF of deterministic CFD simulations for randomly sampled uncertainty parameter as input

Uncertainty Quantification and Safety Factors

Traditional approach to risk management: safety factors

- ❑ Deterministic value is estimated for the load xR (*requirement*) and a value is provided, as best as possible, for the maximum *capacity* xC
  - ❑ On basis of which a safety factor k=xC/xR is imposed on the system

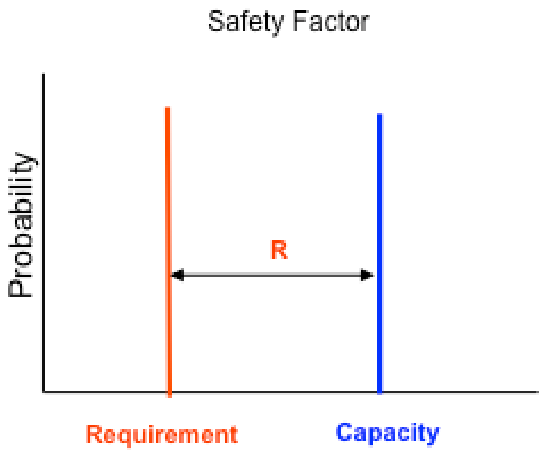

- ❑ Taking the safety factor at a sufficiently high value minimizes risk
  - ❑ This will generally have detrimental consequences on cost and performance

Uncertainty Quantification and Safety Factors

Traditional approach to risk management: safety factors

- ❑ Considering uncertainties and their PDF's
  - ❑ Allows ranges (under the form of PDF's) for requirements (loads) and capacity (resistance) to be evaluated in a rational way
  - ❑ Allows to define a failure region where the two PDF's overlap. Full safety, taking into account the known uncertainties, is obtained for k>1

k>1, the design is perfectly safe (top)

k≅1, a certain risk factor will exist (middle)

k<1, a large failure region exists, which would lead to a catastrophic design, of course to be rejected (bottom)

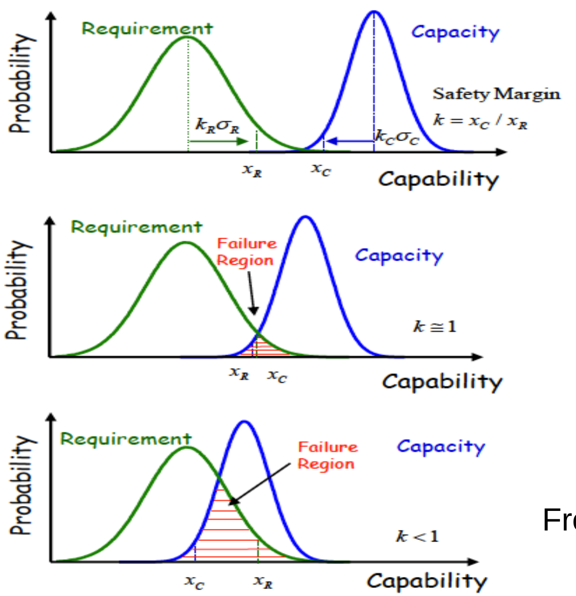

From: Green (2011)

Outline

- ❑ Context
- ❑ **UQ tool for simultaneous operational and geometrical uncertainties implemented in FINE^{TM}**
- ❑ Application of Uncertainty Quantification in Industrial Applications
- ❑ Perspective

Probabilistic collocation method in FINE™ (1/2)

- Non-intrusive probabilistic collocation method by Loeven (2010)
  - Generic stochastic partial differential equation

$$L(a(\theta))u(\vec{x},t,\theta) = S(\vec{x},t) \qquad (1)$$

    - *L* being a differential operator containing space and time derivatives
    - *S* the source terms
    - *a(θ)* the random input parameter
    - *u* the solution which depends on outcome of *θ*
  - Lagrange interpolating polynomials are used to construct the expansion:

$$u(\vec{x},t,\xi(\theta)) = \sum_{i=1}^{N_p} u_i(\vec{x},t) h_i(\xi(\theta)) \qquad (2)$$

    - $u(\vec{x},t,\xi(\theta))$ denotes the deterministic solution
    - $h_i(\xi(\theta))$ Lagrange interpolation polynomial corresponding at collocation point ξ_i

Probabilistic collocation method in FINE™ (2/2)

- Lagrange interpolating polynomial is given by:

$$h_i(\xi) = \prod_{\substack{k=1 \\ k \neq 1}}^{N_p} \frac{\xi - \xi_k}{\xi_i - \xi_k} \qquad (3)$$

  - where $h_i(\xi_i) = \delta_{ij}$

- The collocation points are selected by a Gauss quadrature by means of Golub-Welsch algorithm [Golub (1969)]

$$Q^{(1)} f = \sum_{k=1}^{N} f(\xi_k)\omega_k$$

- To propagate the input uncertainty the expansion (2) is introduced into (1) providing a system of *N* uncoupled simulations

$$L(a(\xi_i))u_i(\vec{x},t) = S(\vec{x},t) \qquad (4)$$

- Once all *N* simulations are computed moments of output quantities are calculated from Gauss quadrature with optimal collocation points and weights

Mean: $\mu_\varphi = \sum_{k=1}^{N_p} w_k \varphi_k(\vec{x},t)$

Variance: $\sigma_\varphi^2 = \sum_{k=1}^{N_p} w_k \varphi_k^2(\vec{x},t) - \mu_\varphi^2$

Tensor-product

Multiple simultaneous uncertainties

- 1D quadrature with N points is given by: $Q^{(1)} f = \sum_{i=1}^{N} f(\xi_i)\omega_i$
- Multi-dimensional quadrature is achieved by tensor-products: $Q^{N_{\dim}} f = \left(Q^{(1)} \otimes \cdots \otimes Q^{(N_{\dim})}\right) f$
  - Each point along one direction is multiplied with each point along all other directions
  - The weights are the products of the 1D-rules

- **Example**: 3 point rule in two dimensions
  - Abscissas: $\xi = \{\xi_1, \xi_2, \xi_3\}$
  - Weights: $\omega = \{\omega_1, \omega_2, \omega_3\}$
  - Resulting points and weights are:

$$(x,y) = \begin{Bmatrix} (\xi_1,\xi_1),(\xi_2,\xi_1),(\xi_3,\xi_1), \\ (\xi_1,\xi_2),(\xi_2,\xi_2),(\xi_3,\xi_2), \\ (\xi_1,\xi_3),(\xi_2,\xi_3),(\xi_3,\xi_3) \end{Bmatrix} \quad \omega = \begin{Bmatrix} \omega_1\omega_1, \omega_2\omega_1, \omega_3\omega_1, \\ \omega_1\omega_2, \omega_2\omega_2, \omega_3\omega_2, \\ \omega_1\omega_3, \omega_2\omega_3, \omega_3\omega_3 \end{Bmatrix}$$

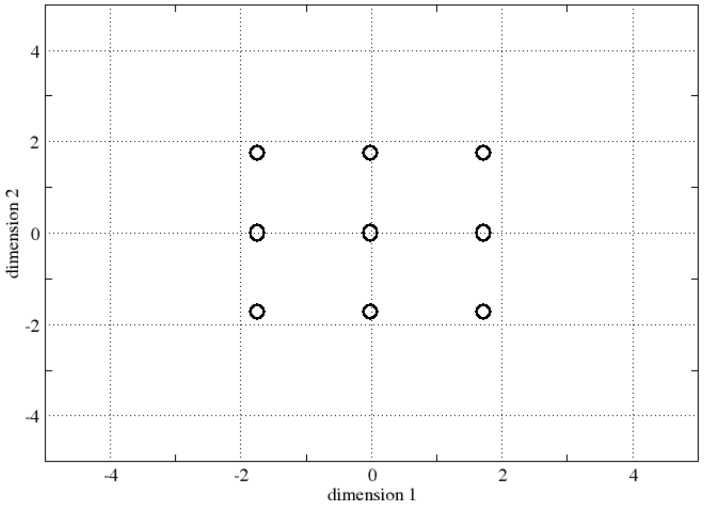

Curse of dimensionality

Exponential growth of cost with number of dimensions

- Number of points created by tensor-product increases exponentially with dimensions
  - 1D-rule with 3 points in 2 dimensions → 9 points = 9 runs of CFD code
  - 1D-rule with 3 points in 3 dimensions → 27 points = 27 runs of CFD code
  - 1D-rule with 3 points in 10 dimensions → 59049 points = 59049 runs of CFD code
  - …
  - 1D-rule with **m** points in **n** dimensions → $\mathbf{m^n}$ points = $\mathbf{m^n}$ runs of CFD code
- This is the so-called "*Curse of dimensionality*".
  - Tensor-products are not feasible for high dimensions
- UMRIDA quantifiable objective: *At least 10 simultaneous uncertainties, in a turn-over time of less than 10 hours on a 100 core parallel computer*
- **Sparse Grids** can overcome this limit to a certain extend and make non-intrusive collocation methods accessible for higher dimensions
  - Sparse grids were proposed by Smolyak (1963)

Smolyak Quadrature

- For different levels of accuracy **k**, define a difference formula: $Q_l^{(1)} f = \sum_{k=1}^{l} \left(Q_k^{(1)} - Q_{k-1}^{(1)}\right) f$
  - where $Q_0^{(1)} f \equiv 0$
- With: $\Delta_k^{(1)} = \left(Q_k^{(1)} - Q_{k-1}^{(1)}\right) f$ we get: $Q_l^{(1)} f = \sum_{k=1}^{l} \Delta_k$
- For multi-dimensional quadrature the order of *summation* and *tensor-product* is changed:

$$Q_l^{N_{\dim}} f = \left(Q_l^{(1)} \otimes \cdots \otimes Q_l^{(N_{\dim})}\right) f = \left(\sum_{k=1}^{l_1} \Delta_k \otimes \cdots \otimes \sum_{j=1}^{l_{\dim}} \Delta_j\right) = \left(\sum_{k=1}^{l_1} \cdots \sum_{j=1}^{l_{\dim}} \left(\Delta_k \otimes \cdots \otimes \Delta_j\right)\right)$$

- The sum can now be truncated to include fewer mixed terms
  - This is done by the use of a multi-index ***K***, which is truncated to a **total order**

$$Q_l^{N_{\dim}} f = \sum_{k \in K} \left(\Delta_k^{(1)} \otimes \cdots \otimes \Delta_k^{(N_{\dim})}\right)$$

Multi-Index

- We can write for two dimensions and level 2: $\sum_{k \in K} a_k = \sum_{i=0}^{2} \sum_{j=0}^{2} a_{ij}$

$$K = \begin{Bmatrix} (0,0),(1,0),(2,0), \\ (0,1),(1,1),(2,1), \\ (0,2),(1,2),(2,2) \end{Bmatrix}$$

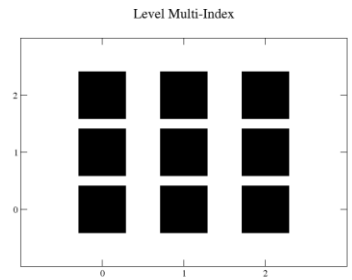

Full index

$$K = \begin{Bmatrix} (0,0),(1,0),(2,0), \\ (0,1),(1,1), \\ (0,2) \end{Bmatrix}$$

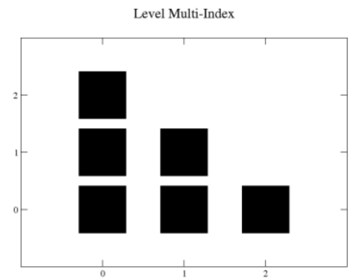

Truncated to total level 2

- For the Smolyak Quadrature: $Q_l^{N_{\dim}} f = \sum_{k \in K} \left(\Delta_k^{(1)} \otimes \cdots \otimes \Delta_k^{(N_{\dim})} \right)$
  - The classical truncation by total index is isotropic and gives: $K = \left\{ k \in N_0^{\dim} : \|k\|_1 \leq l + \dim - 2 \right\}$

Comparison tensor-product to sparse grid

- 2-dimensional grids with *3* and *7* points per 1D-rule

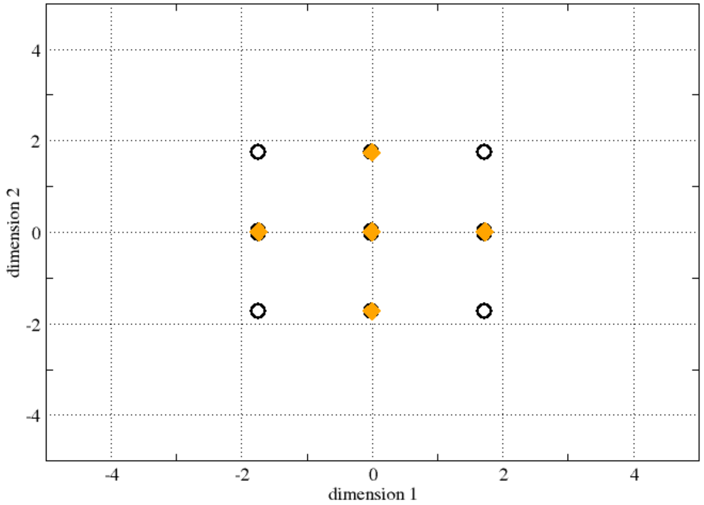

Tensor-Grid: 9
Sparse-Grid: 5

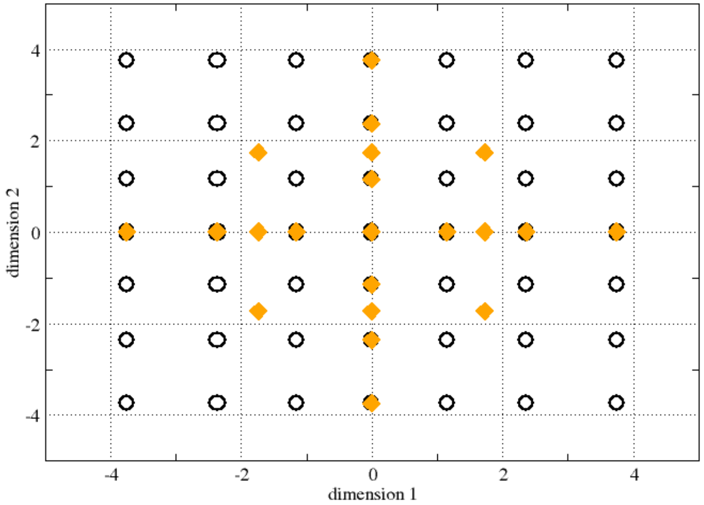

Tensor-Grid: 49
Sparse-Grid: 21

Points for tensor grids and sparse grids with linear and exponential growth

- Sparse grids can be build with linear and exponential growth in number of points per level
  - # points for linear growth: # points = 2 level + 1
  - # points for exponential growth: # points = $2^{\text{level}+1}$ -1
- Important that level zero is mid-point rule for sparse grids!
- Table summarizing different grid sizes

Level	0			1			2			3			4			5		
Dimension	**Tensor**	**Sparse LG**	**Sparse EG**	**Tensor**	**Sparse LG**	**Sparse EG**	**Tensor**	**Sparse LG**	**Sparse EG**	**Tensor**	**Sparse LG**	**Sparse EG**	**Tensor**	**Sparse LG**	**Sparse EG**	**Tensor**	**Sparse LG**	**Sparse EG**
1	2	1	1	3	3	3	4	5	7	5	7	15	6	9	31	7	11	63
2	4	1	1	9	5	5	16	17	21	25	45	73	36	97	221	49	181	609
3	8	1	1	27	7	7	64	31	37	125	105	159	216	297	597	343	735	2031
4	16	1	1	81	9	9	256	49	57	625	201	289	1296	681	1265	2401	2001	4969
5	32	1	1	243	11	11	1024	71	81	3125	341	471	7776	1341		16807		
...	...	...	...	...	...	...	...	...	...	...	...	...	...	...	...	...	...	...
10	1024	1	1	59049	21	21	1048576	241	261	9765625	1981	2441	60466176	12981		282475249		

- For a given 1D-accuracy exponential growth sparse grid has fewest points

Handling operational uncertainties – Selection from GUI

- ❑ Selection of operational uncertainties by simple selection from boundary conditions

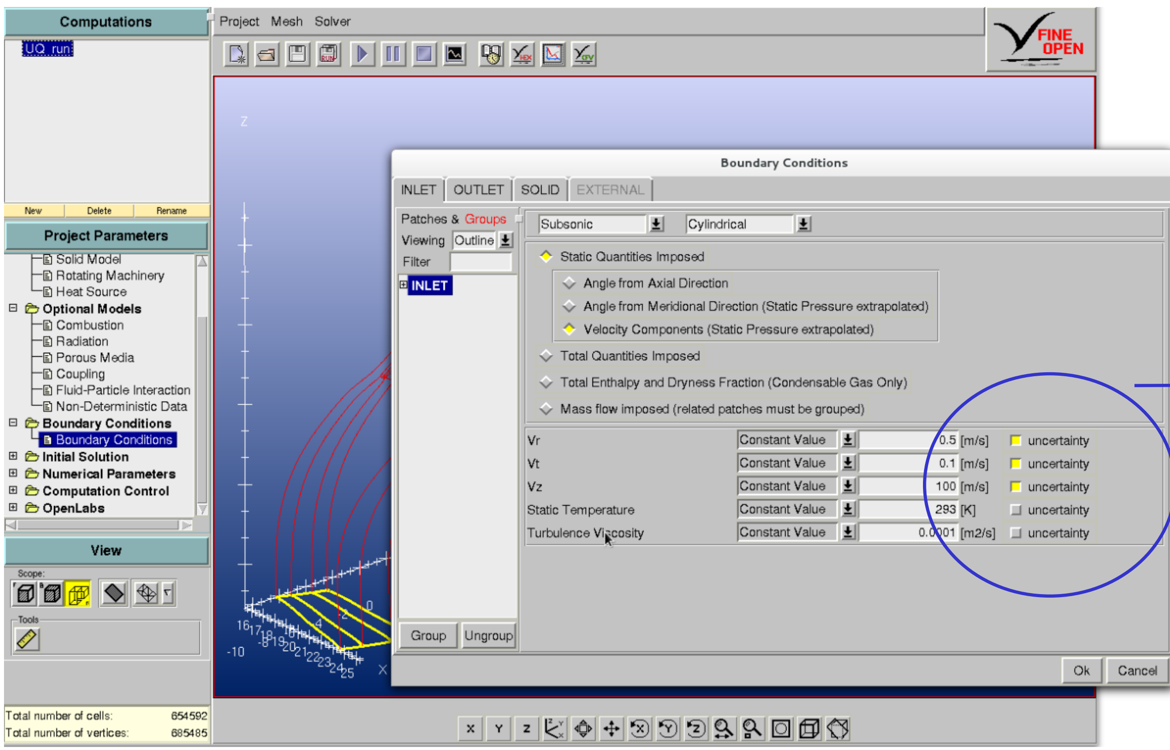

Select operational parameter subject to uncertainties by simple click

UQ tool for operational and geometrical uncertainties

Handling operational uncertainties – Automatic generation of computations

- Tensor-product or Sparse Grids are used to calculate entries for sub-computations

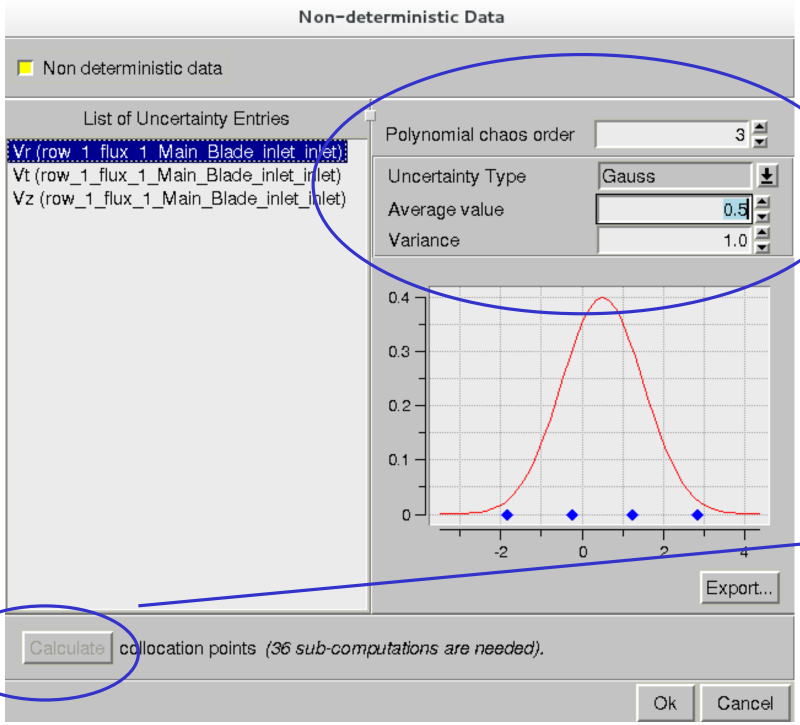

Define type and values of PDF to be imposed through a dedicated GUI window

Calculation of collocation points and **automatic generation** of individual non-deterministic simulations:

- Tensor-product
- Sparse Grids

UQ tool for operational and geometrical uncertainties

Geometrical uncertainties require modification of the geometry!!!

- ❑ Need a platform that allows for automatic parameterization of geometry, meshing and simulation set-up

- ❑ Combined operational and geometrical uncertainties based on optimization tool FINE™/Design
  - ❑ This allows also for a natural extension to optimization under uncertainties

- ❑ UQ module is introduced on this basis, which controls parameterization of geometry, meshing and simulation set-up

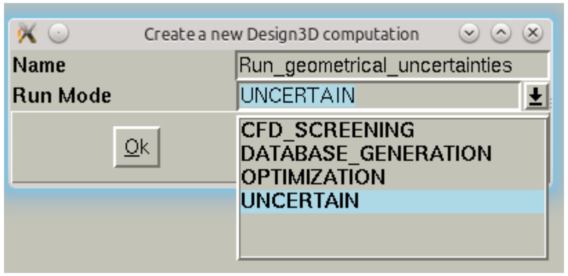

UQ tool for operational and geometrical uncertainties

Selection of design parameters through GUI

- All design parameters can be combined with uncertainties
- Even new parameters can be added, such as the tip gap

LEAN_BETA1	-2.2324952064	-0.2324952064	1.76750479356	1	Uncertainty
LEAN_BETA2	-2.7720933921	-0.7720933921	1.22790660782	1	Uncertainty
NB	36	36	36	2	Uncertainty
BLADE_ROTATION	0.08761070082	0.08761070082	0.08761070082	1	Uncertainty
TIP_GAP	0	0.000356	0.001	1	Uncertainty
S1_LE_R_NOM	0.00012285585	0.00012285585	0.00012285585	1	Uncertainty
S2_LE_R_NOM	8.70765922148	8.70765922148	8.70765922148	1	Uncertainty
S3_LE_R_NOM	3.04267736287	3.04267736287	3.04267736287	1	Uncertainty
S1_TE_R_NOM	0.00021949334	0.00021949334	0.00021949334	1	Uncertainty
S2_TE_R_NOM	0.00011880032	0.00011880032	0.00011880032	1	Uncertainty
S3_TE_R_NOM	9.17886681025	9.17886681025	9.17886681025	1	Uncertainty
TE_VARIATION	-10	1	10	1	Uncertainty
LE_VARIATION	-10	1	10	1	Uncertainty

UQ tool for operational and geometrical uncertainties

Selection of product rule and uncertainty type from GUI

- ❑ All parameters can be selected and suitable PDF can be attributed
- ❑ Computations with **different geometries and meshes are automatically generated**

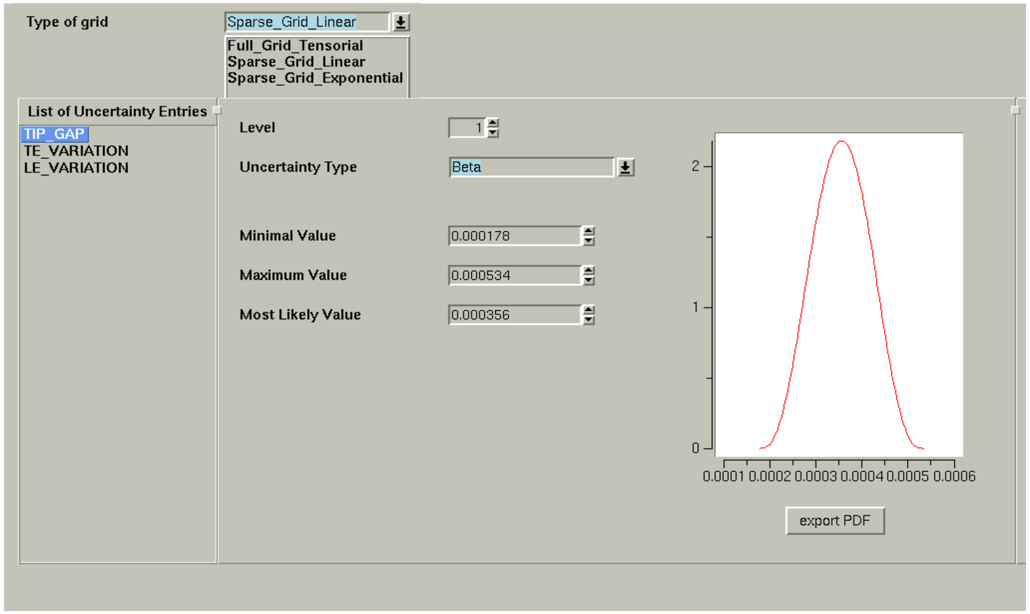

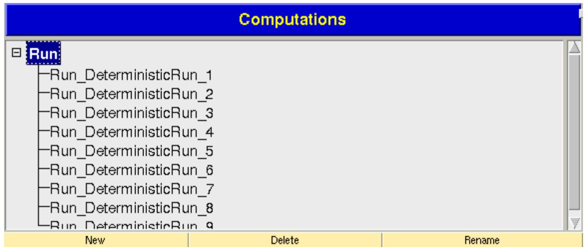

Automatic generation of sub-computations with different geometries and boundary conditions

UQ tool for operational and geometrical uncertainties

Post-treatment of non-deterministic simulations

- ❑ First four moments of selected scalar output quantities are calculated automatically

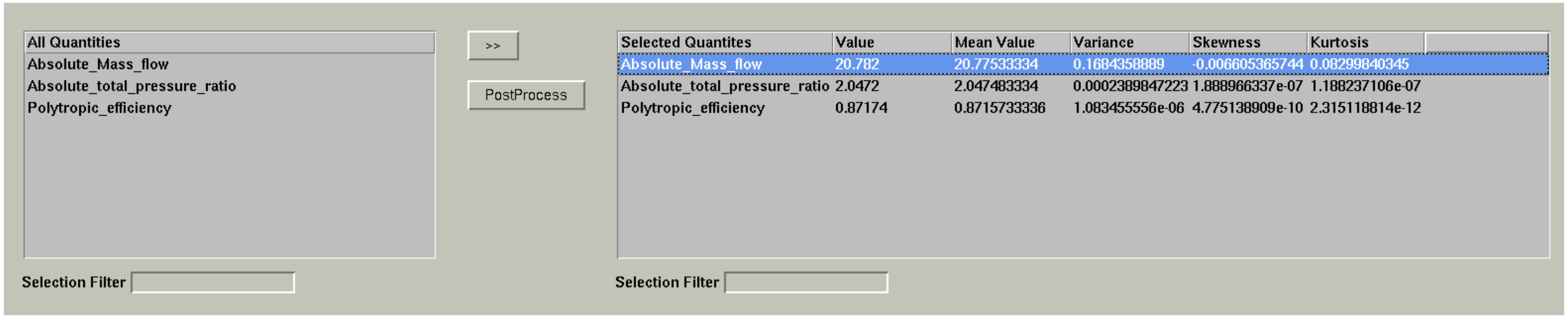

Selected Quantites	Value	Mean Value	Variance	Skewness	Kurtosis
Absolute_Mass_flow	20.782	20.77533334	0.1684358889	-0.006605365744	0.08299840345
Absolute_total_pressure_ratio	2.0472	2.047483334	0.0002389847223	1.888966337e-07	1.188237106e-07
Polytropic_efficiency	0.87174	0.8715733336	1.083455556e-06	4.775138909e-10	2.315118814e-12

- ❑ Visualization of performance curve for turbo-machinery applications with uncertainty bars

- ❑ Reconstruction of PDFs based on first four output moments (Pearson method)

Output of non-deterministic simulations

Probability distribution function (PDF) of output quantities

- Performing non-deterministic simulations
  - The output is not a single number anymore but a PDF
  - From the example of Monte-Carlo simulations it becomes obvious that the output of non-deterministic simulations is a PDF

Sampling a high number of realizations

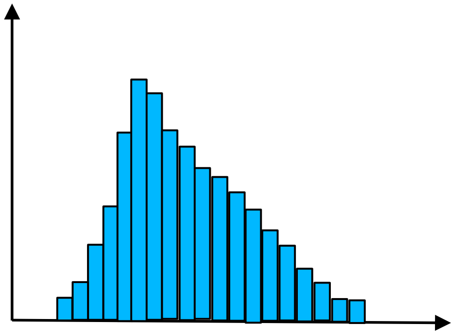

- How his this information provided by the here used probabilistic collocation method or by moment methods?
  - PDF of output quantities is characterized by the moments of the output quantity

Output of non-deterministic simulations

Statistical moments of a PDF

- Influence of Variance (or standard deviation σ²=Var(X))
- Influence of Skewness

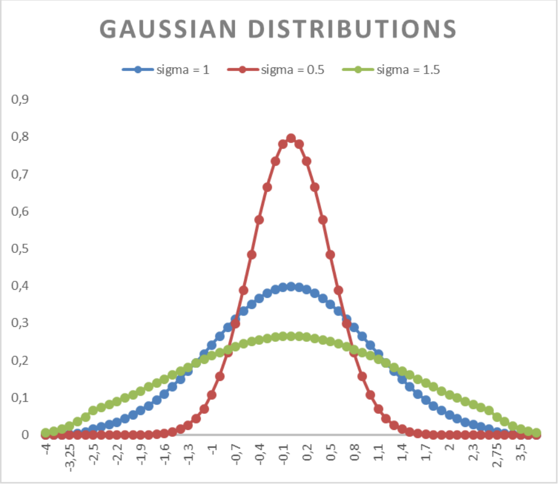

Mean $$\mu_\varphi = \sum_{k=1}^{N_p} w_k \varphi_k(\vec{x},t)$$

Variance (standard deviation) $$\sigma_\varphi^2 = \sum_{k=1}^{N_p} w_k \varphi_k^2(\vec{x},t) - \mu_\varphi^2$$

Skewness $$\sum_{k=1}^{N_p} w_k \varphi_k^3(\vec{x},t) - \mu_\varphi^3$$

Kurtosis $$\sum_{k=1}^{N_p} w_k \varphi_k^4(\vec{x},t) - \mu_\varphi^4$$

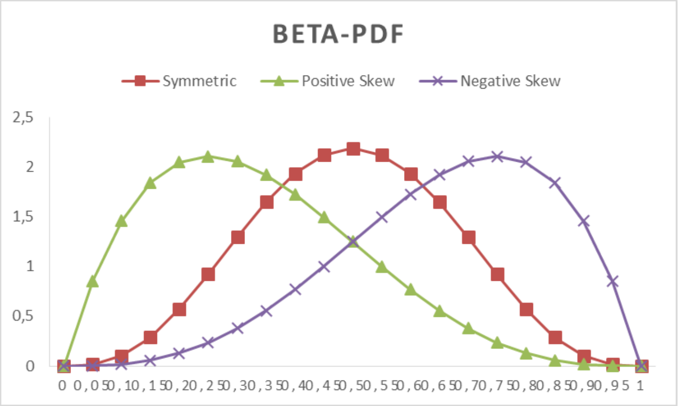

Output of non-deterministic simulations

How to obtain from the moments of a PDF to the PDF itself

- ❑ Based on these statistical moments a PDF can be reconstructed by PEARSON system [Pearson (1895)]

Mean $\mu_\varphi = \sum_{k=1}^{N_p} w_k \varphi_k(\vec{x},t)$

Variance (standard deviation) $\sigma_\varphi^2 = \sum_{k=1}^{N_p} w_k \varphi_k^2(\vec{x},t) - \mu_\varphi^2$

Skewness $\sum_{k=1}^{N_p} w_k \varphi_k^3(\vec{x},t) - \mu_\varphi^3$

Kurtosis $\sum_{k=1}^{N_p} w_k \varphi_k^4(\vec{x},t) - \mu_\varphi^4$

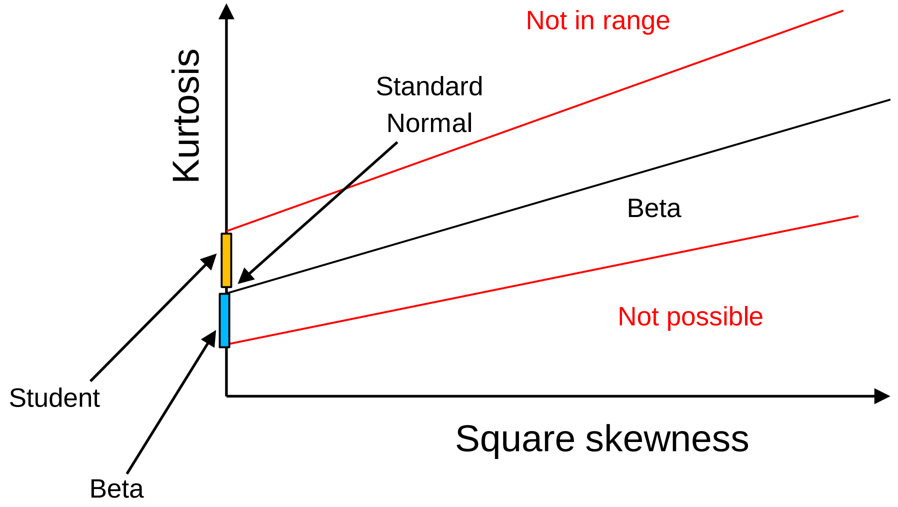

Following: Roge G (2013)

Output of non-deterministic simulations

How to obtain from the moments of a PDF to the PDF itself

- Verification of reconstruction on known PDF shape

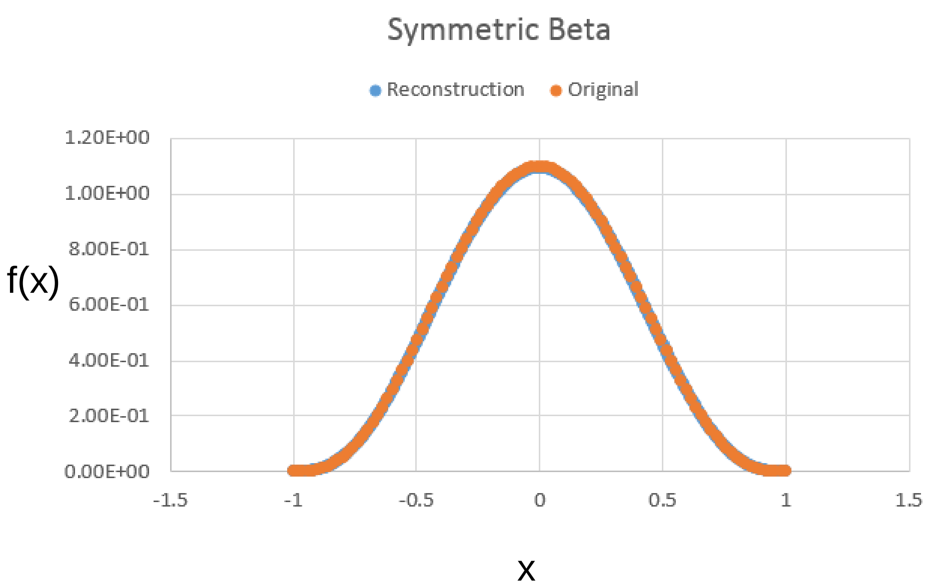

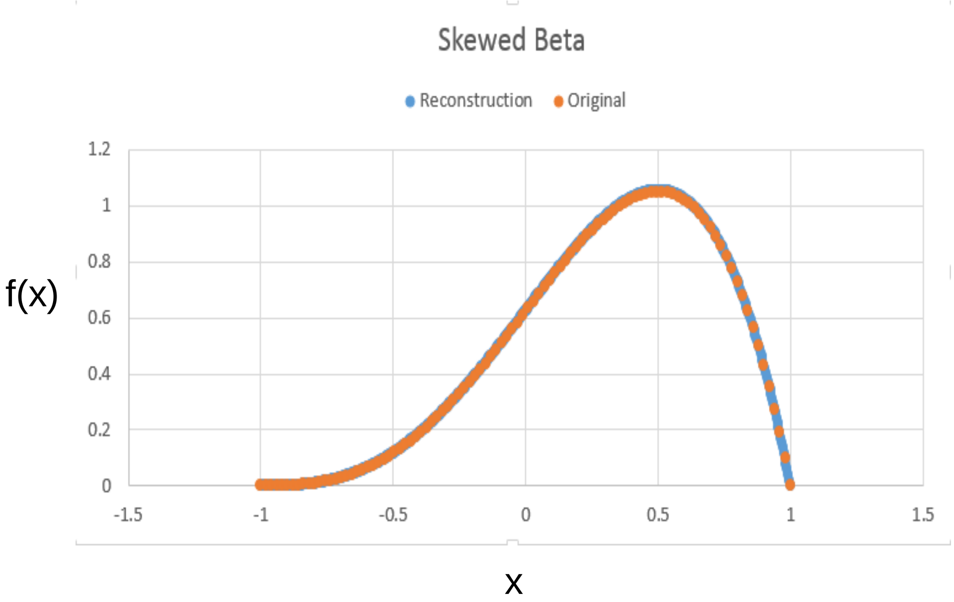

Level of collocation method

Which level is needed for the collocation method

- ❑ Increasing level leads to higher computational cost

Level	0			1			2			3			4			5		
Dimension	**Tensor**	**Sparse LG**	**Sparse EG**	**Tensor**	**Sparse LG**	**Sparse EG**	**Tensor**	**Sparse LG**	**Sparse EG**	**Tensor**	**Sparse LG**	**Sparse EG**	**Tensor**	**Sparse LG**	**Sparse EG**	**Tensor**	**Sparse LG**	**Sparse EG**
1	2	1	1	3	3	3	4	5	7	5	7	15	6	9	31	7	11	63
2	4	1	1	9	5	5	16	17	21	25	45	73	36	97	221	49	181	609
3	8	1	1	27	7	7	64	31	37	125	105	159	216	297	597	343	735	2031
4	16	1	1	81	9	9	256	49	57	625	201	289	1296	681	1265	2401	2001	4969
5	32	1	1	243	11	11	1024	71	81	3125	341	471	7776	1341		16807		
…	…	…	…	…	…	…	…	…	…	…	…	…	…	…	…	…	…	…
10	1024	1	1	59049	21	21	1048576	241	261	9765625	1981	2441	60466176	12981		282475249		

- ❑ To which order should the expansion be truncated?
  - ❑ The required order is controlled by the random variable which is represented (flow solution), particularly its probability law
  - ❑ This is however not known a priori, but the law associated with the input uncertainties is known
  - ❑ The error by truncating the expansion to a given order must be evaluated for statistical output moments
  - ❑ Unfortunately, the computation cost increases with increasing order

Outline

- ❑ Context
- ❑ UQ tool for simultaneous operational and geometrical uncertainties implemented in FINE^{TM}
- ❑ **Application of Uncertainty Quantification in Industrial Applications**
- ❑ Perspective

Application to Rotor 37

Test case description: Rotor 37

- ❑ Detailed description of geometry, exp. set-up and a series of simulations cross-plotting the predictions can be found in [Dunham (1998)]

- ❑ Test case and UQ model
  - ❑ Mesh size: 2 639 973 and 4 702 629 cells
  - ❑ RANS + Spalart-Allmaras
  - ❑ Rotating Hub: 17188 rpm
  - ❑ Use of CPU-Booster in FINE^{TM}/Turbo

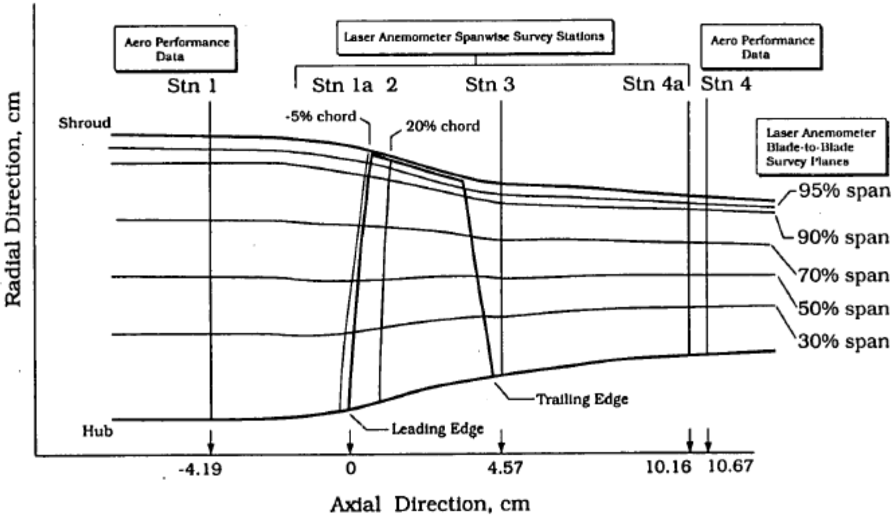

- ❑ Uncertainties: all PDFs are Gaussian
  1. 5 uncertainties: total inlet pressure, static outlet pressure, tip gap, LE angle, TE angle
  2. 9 uncertainties: total inlet pressure, static outlet pressure, tip gap, LE angle (3 sections), TE angle (3 sections)

Application to Rotor 37

Overview of imposed uncertainties

- ❑ Operational and Geometrical uncertainties

Uncertainty	Most likely value (m)	Minimum value (a)	Maximum value (b)	PDF-type
Inlet total pressure	Table at station 1 in [1]	98% m	102% m	Symmetric beta-PDF
Static outlet pressure	Table 1 below	98% m	102% m	Symmetric beta-PDF

Uncertainty	Most likely value (m)	Minimum value (a)	Maximum value (b)	PDF-type
Tip clearance	M_{tip}=0.356mm	50% M_{tip}	150% M_{tip}	Symmetric beta-PDF
Leading edge angle	LE_{angle}=5	95% LE_{angle}	105% LE_{angle}	Symmetric beta-PDF
Trailing edge angle	TE_{angle}=-70	95% TE_{angle}	105% TE_{angle}	Symmetric beta-PDF

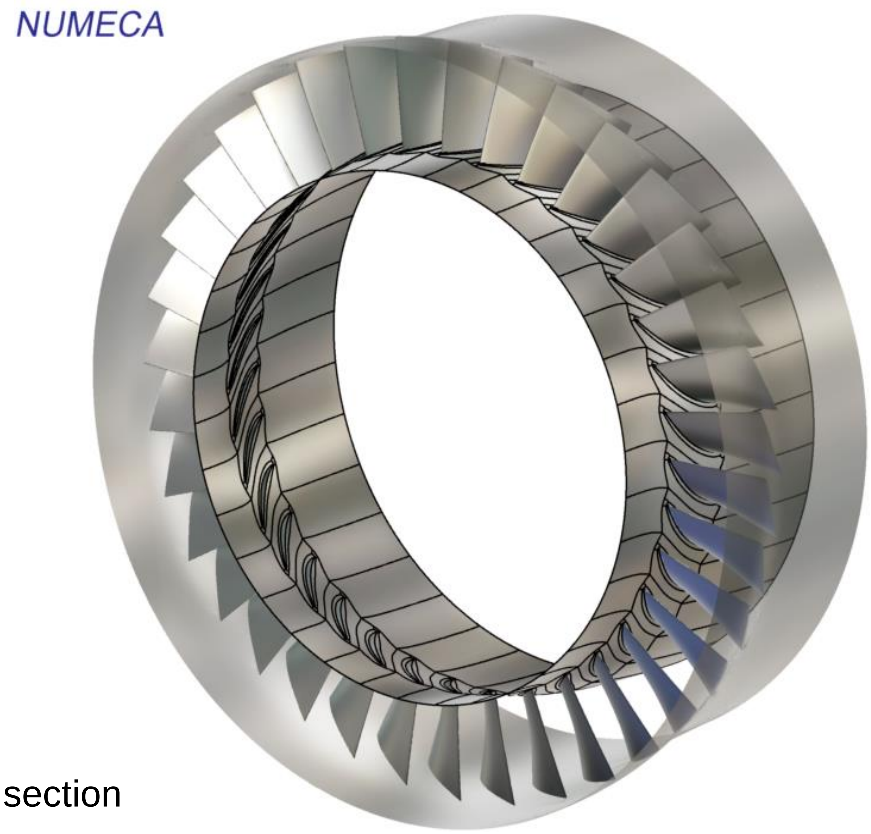

- ❑ 5 uncertainties: LE and TE variation identical for each section
- ❑ 9 uncertainties: LE an TE variation is different for 3 sections

Automatic generation of meshes with varying tip gap

- Same mesh size for <u>automatically</u> generated geometries with **varying tip gap**

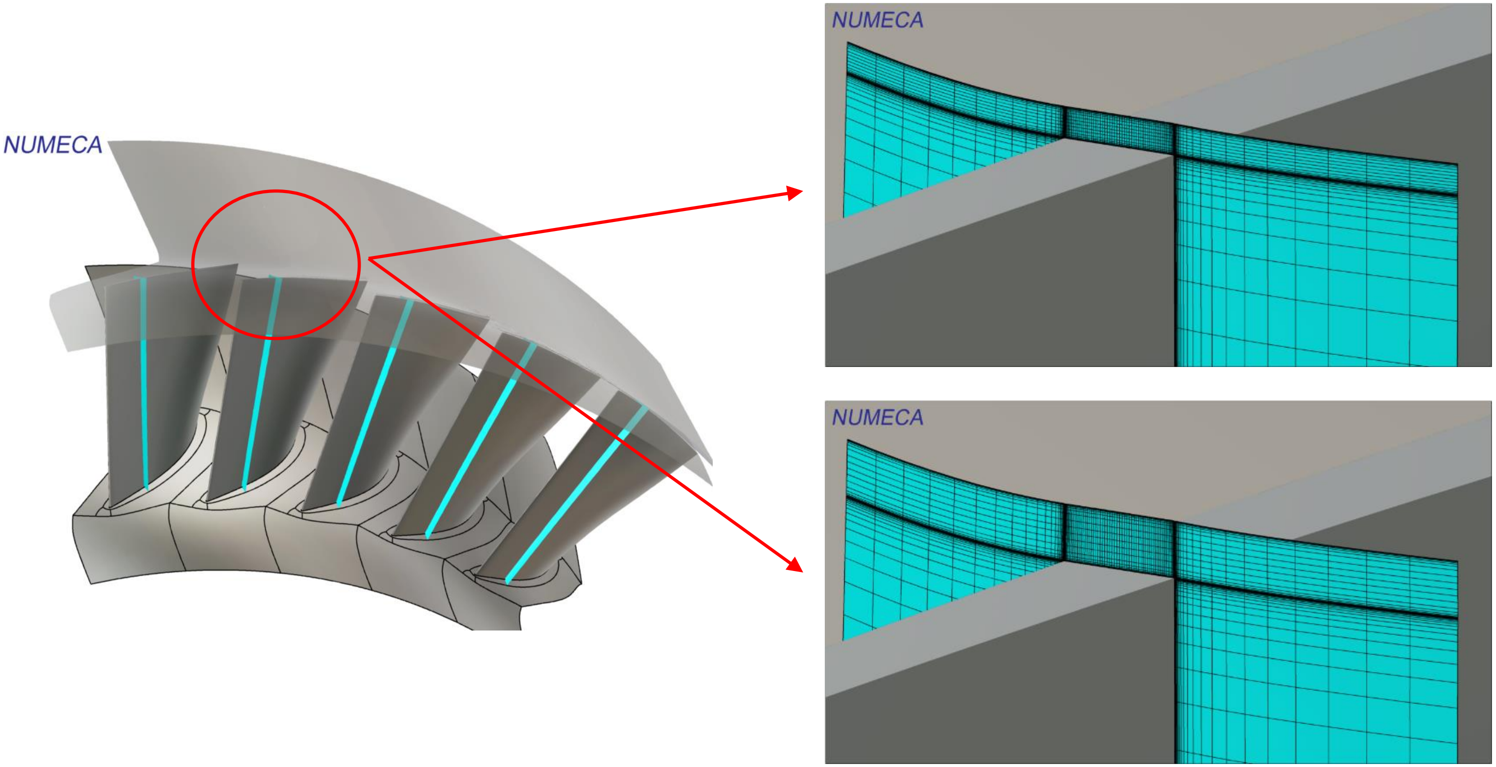

Smallest tip gap

Largest tip gap

Application to Rotor 37

Automatic generation of meshes with varying trailing edge angle

- ❑ Same mesh size for <u>automatically</u> generated geometries with **varying TE angle**

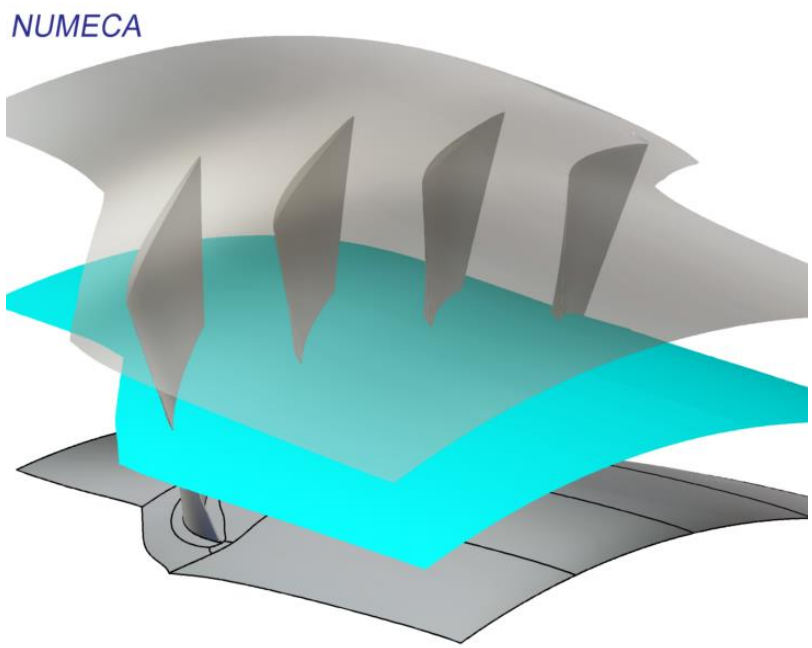

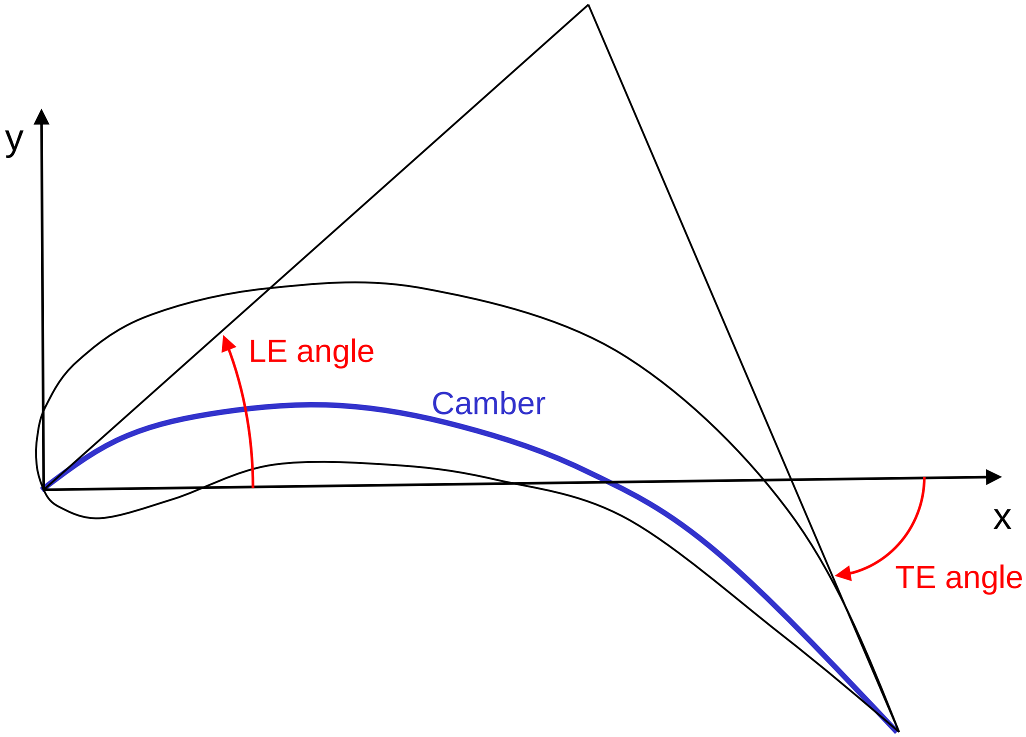

Automatic generation of meshes with varying trailing edge angle

- ❑ Same mesh size for <u>automatically</u> generated geometries with **varying TE angle**

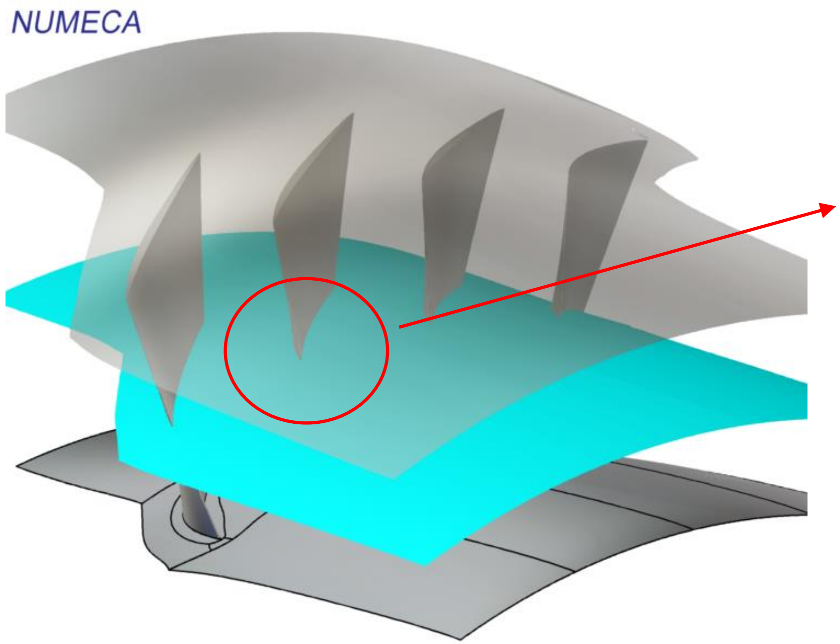

Smallest angle

Largest angle

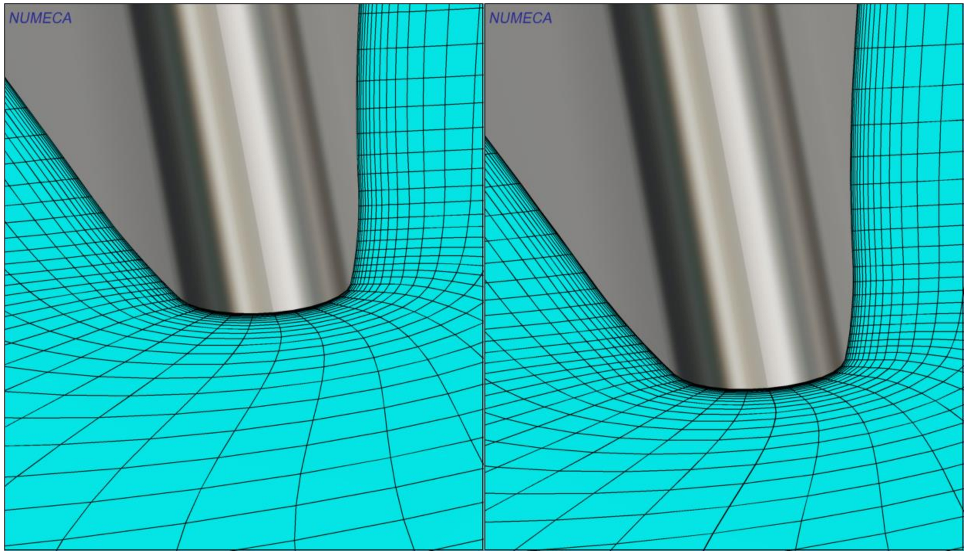

Application to Rotor 37

Validation of UQ approach

Level	0			1			2			3			4			5		
Dimension	**Tensor**	**Sparse LG**	**Sparse EG**	**Tensor**	**Sparse LG**	**Sparse EG**	**Tensor**	**Sparse LG**	**Sparse EG**	**Tensor**	**Sparse LG**	**Sparse EG**	**Tensor**	**Sparse LG**	**Sparse EG**	**Tensor**	**Sparse LG**	**Sparse EG**
1	2	1	1	3	3	3	4	5	7	5	7	15	6	9	31	7	11	63
2	4	1	1	9	5	5	16	17	21	25	45	73	36	97	221	49	181	609
3	8	1	1	27	7	7	64	31	37	125	105	159	216	297	597	343	735	2031
4	16	1	1	81	9	9	256	49	57	625	201	289	1296	681	1265	2401	2001	4969
5	32	1	1	243	11	11	1024	71	81	3125	341	471	7776	1341		16807		
...	...	...	...	...	...	...	...	...	...	...	...	...	...	...	...	...	...	...
9	512	1	1	19683	19	19	262144	199	217	1953125	1501	1879	...	...	...	...	...	...
10	1024	1	1	59049	21	21	1048576	241	261	9765625	1981	2441	60466176	12981	...	282475249	...	...

Presented simulations

Additional simulations

❑ Validation of UQ approach

1. Tensor-product with sparse grids
2. Parametric uncertainty model with 5 and 9 uncertainties
3. Influence of number of points per 1D direction and growth rate

Validation UQ approach: Tensor-product to Sparse Grid

- Simulation with 5 uncertainties
  - TE and LE edge angle constant along radius
  - TE and LE edge angle with Gaussian PDF
  - Full tensor-product (243 runs)
  - Linear growth sparse grid (11 runs)

Full/sparse	Mean	Variance
Absolute_Mass_flow	1,00013	0,993831485
Absolute_total_pressure_ratio	1,000029	0,990279725

- Mean and Variance are almost identical
  - Validity of Sparse Grid compared to tensor-product
  - Sparse Grid provides same results with 22 times less simulations
  - CPU time for one computation on 6 parallel processors approx. 25 minutes: 1,5 CPUh
  - Total reduction in CPU time from approximately **364.5 CPUh to 16.5 CPUh**

Non-deterministic analysis: overview

- Simulation characteristics
  - Mesh independent solution with 4 702 629 cells
  - RANS + Spalart-Allmaras
  - Rotating Hub: 17188 rpm
  - Use of CPU-Booster in FINE™/Turbo

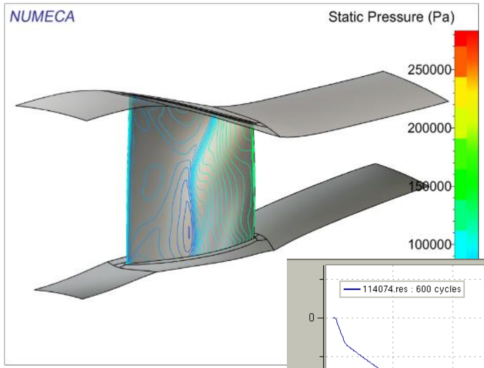

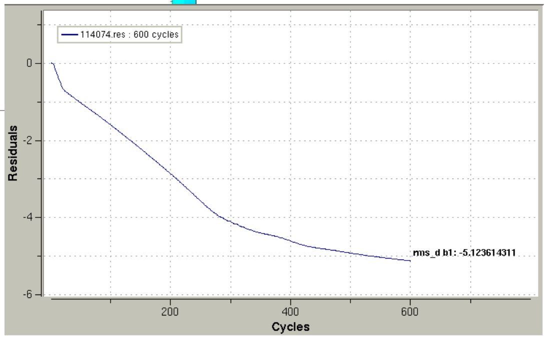

- UQ characteristics

Uncertainty	Most likely value (m)	Minimum value (a)	Maximum value (b)	PDF-type
Tip clearance	M_{tip}=0.356mm	50% M_{tip}	150% M_{tip}	Symmetric beta-PDF
Leading edge angle	LE_{angle}=5	95% LE_{angle}	105% LE_{angle}	Symmetric beta-PDF
Trailing edge angle	TE_{angle}=-70	95% TE_{angle}	105% TE_{angle}	Symmetric beta-PDF

Uncertainty	Most likely value (m)	Minimum value (a)	Maximum value (b)	PDF-type
Inlet total pressure	Table at station 1 in [1]	98% m	102% m	Symmetric beta-PDF
Static outlet pressure	Table 1 below	98% m	102% m	Symmetric beta-PDF

Non-deterministic analysis: C_p on blade surface - UQ

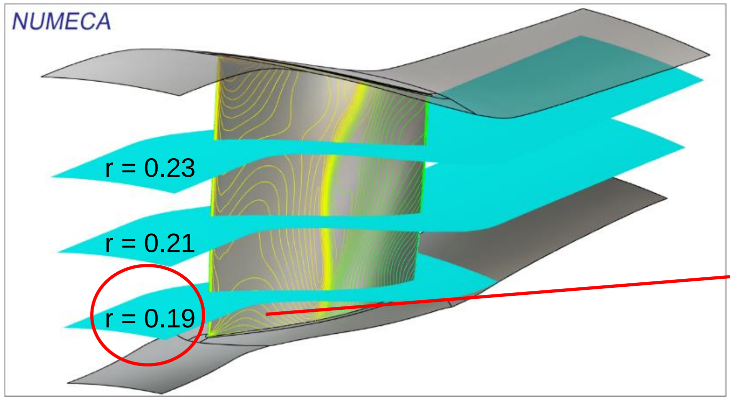

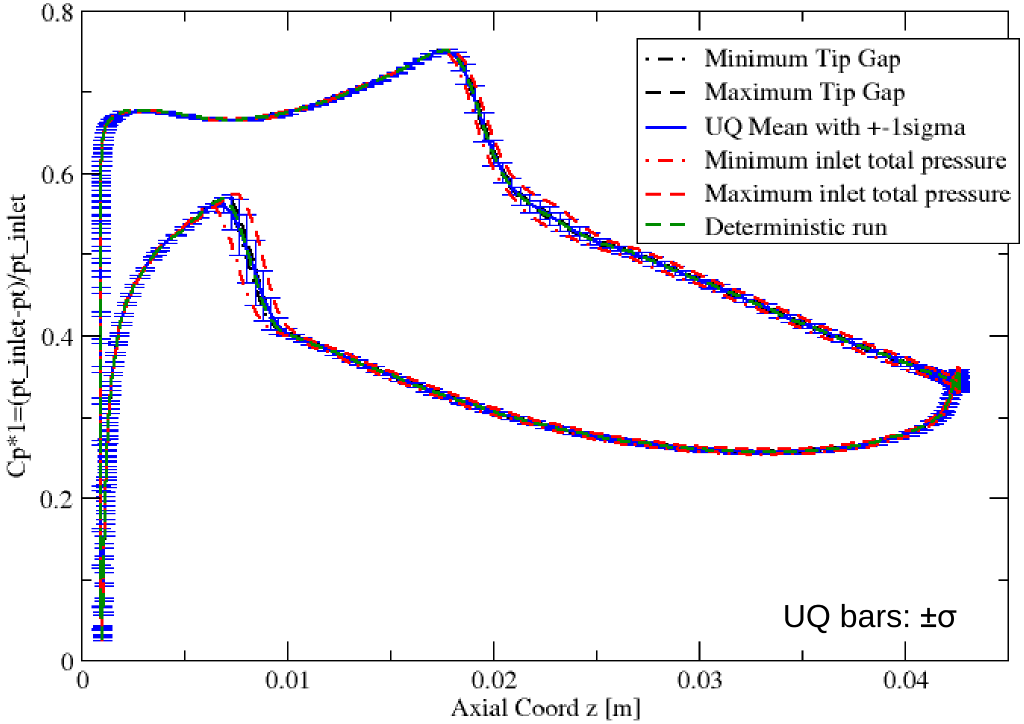

- Solution is now a PDF represented by its first two statistical moments
- Individual non-deterministic sub-computations provide some kind of sensitivity
- Uncertainty in solution is the largest in the near shock region

Non-deterministic analysis: C_p on blade surface – UQ and Sensitivity

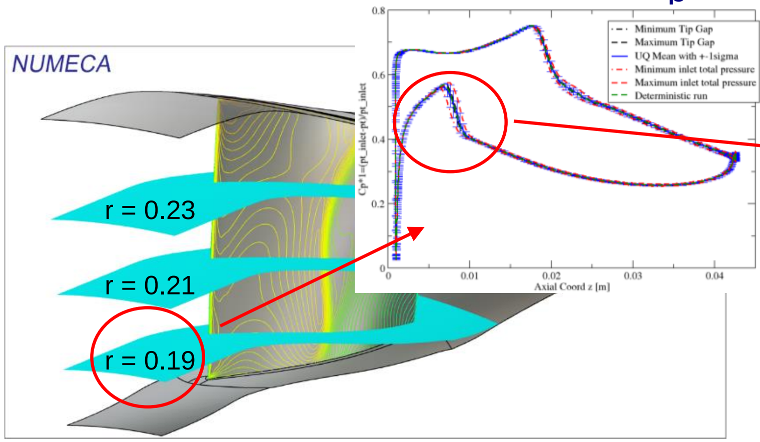

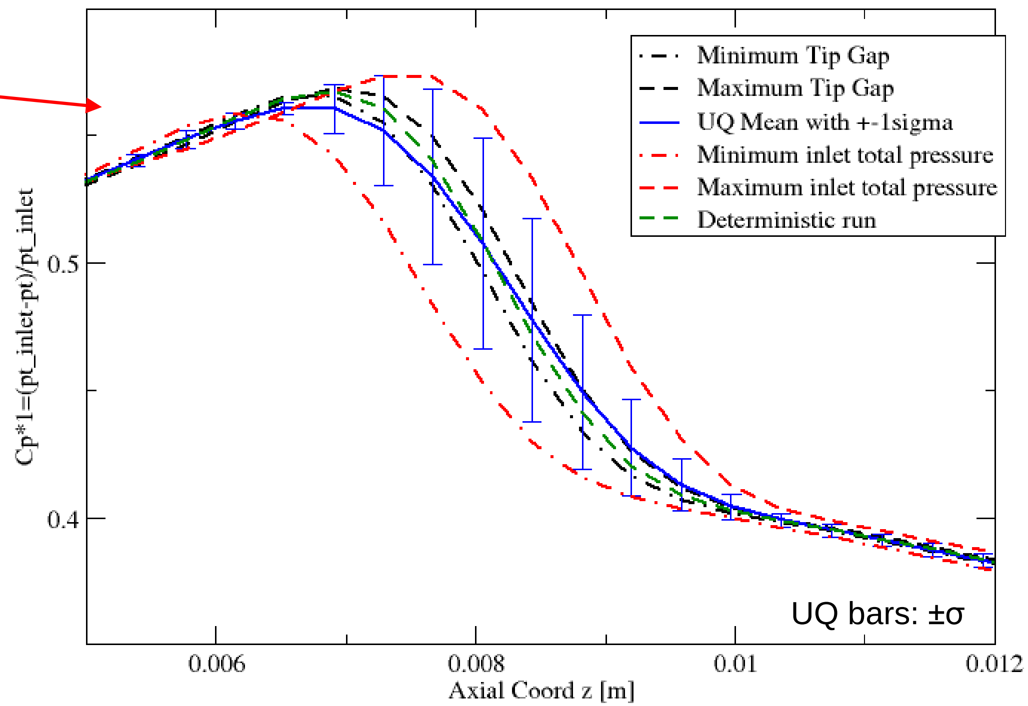

- Individual non-deterministic sub-computations provide some kind of sensitivity
- Influence of inlet total pressure much stronger on uncertainties in shock region compared to tip gap
- This kind of evaluation can be conducted for any flow phenomenon of interest

Non-deterministic analysis: C_p on blade surface – Comparison radial cuts

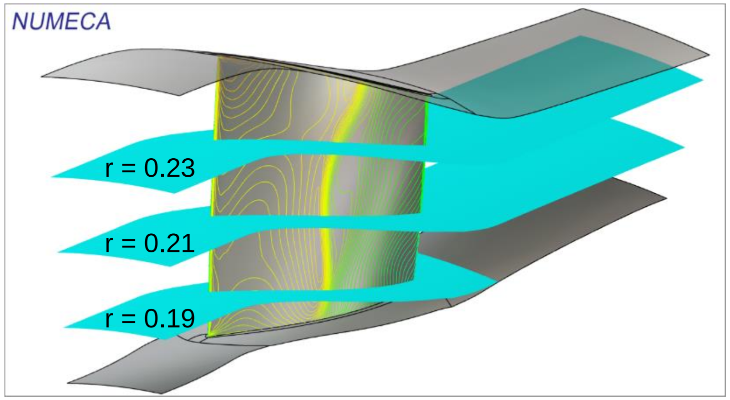

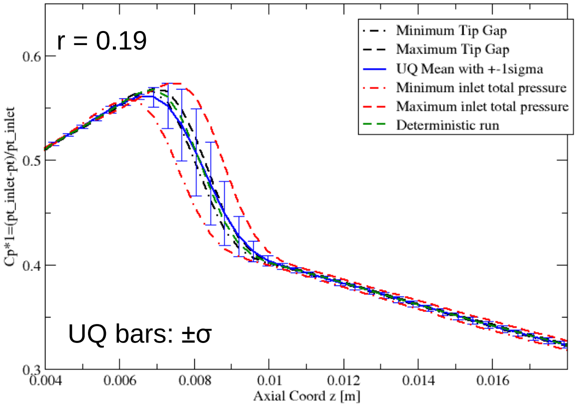

- Uncertainties at different span wise locations
- Not only the deterministic and non-deterministic mean are different, but non-deterministic results is a PDF instead of a single value

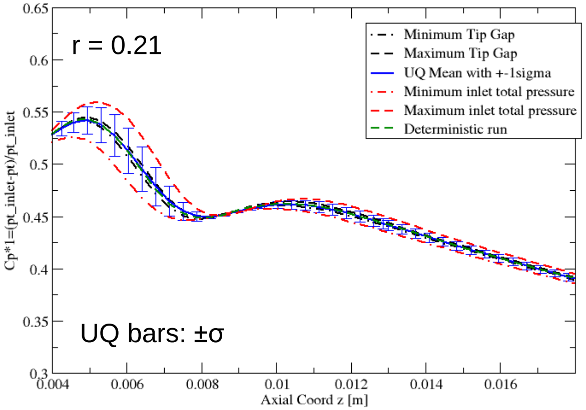

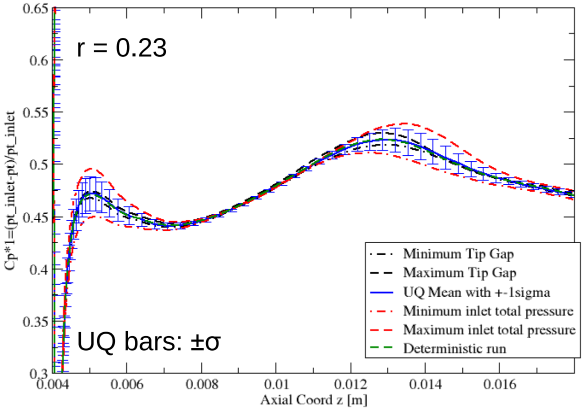

Application to Rotor 37

Non-deterministic analysis: pitch-wise averaged total pressure ratio

- Pitch-wise averaged at computation domain outlet

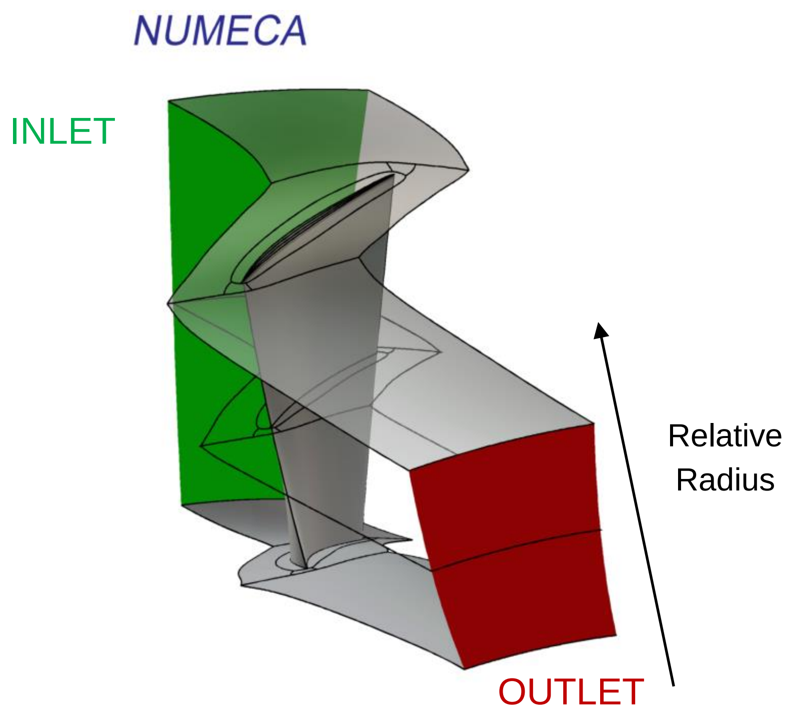

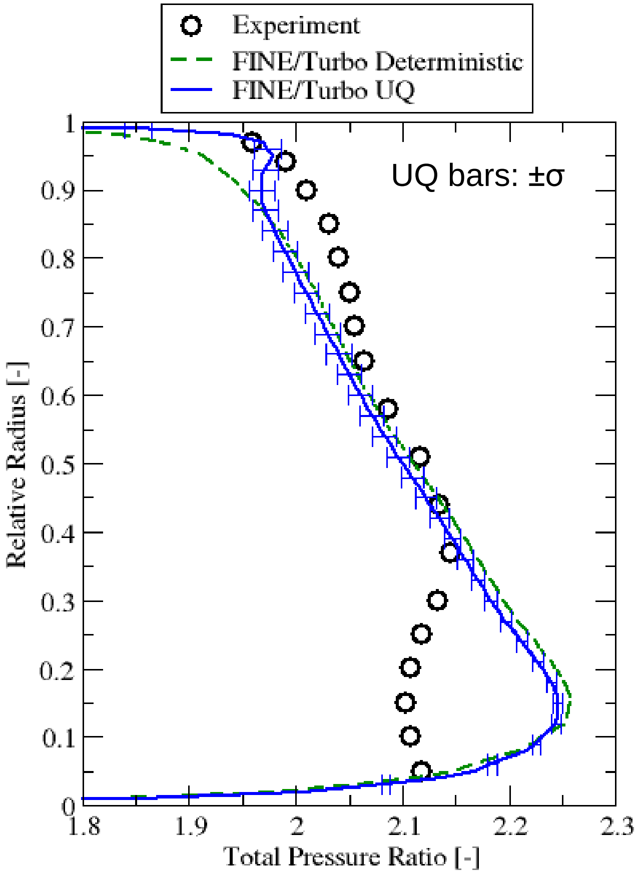

Non-deterministic analysis: pitch-wise averaged total temperature ratio

- Pitch-wise averaged at computation domain outlet

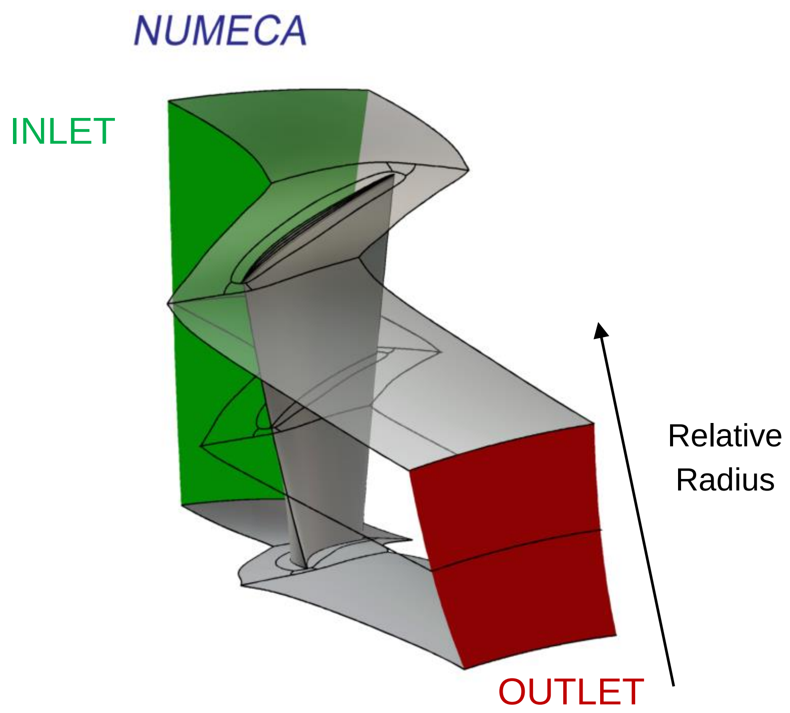

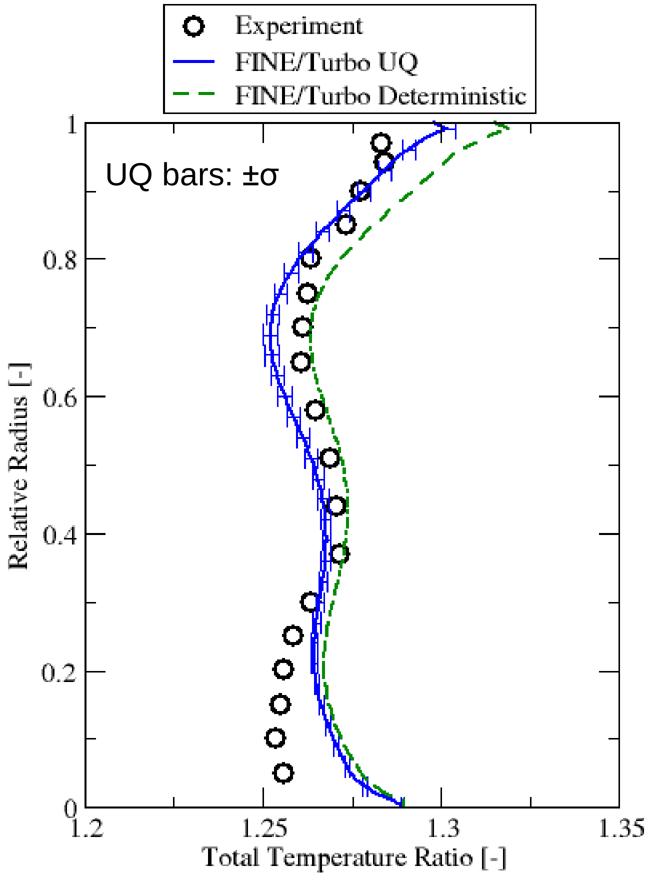

Application to Rotor 37

Non-deterministic analysis: Compressor map

- Little influence of LE/TE discretization (5 or 9 uncertainties)
- Non-deterministic simulations results are given by a PDF not by a single value
- This PDF is here represented by UQ bars

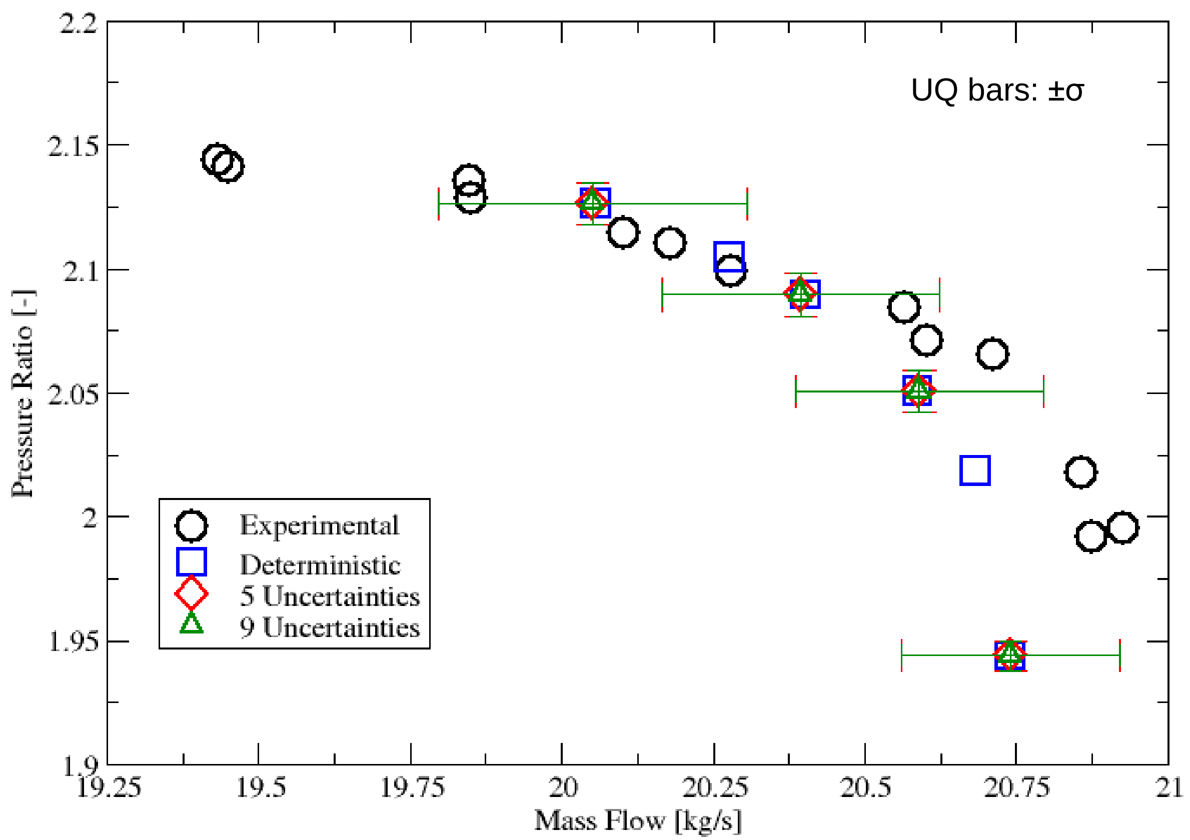

Non-deterministic analysis: Compressor map with only static outlet pressure as uncertain variable

- Only the static outlet pressure as uncertainty

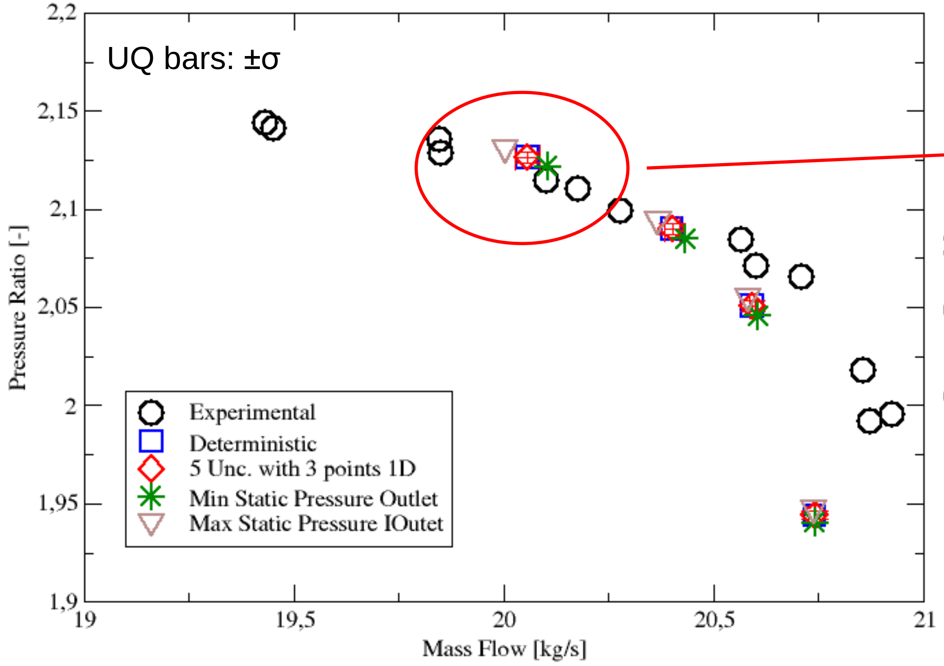

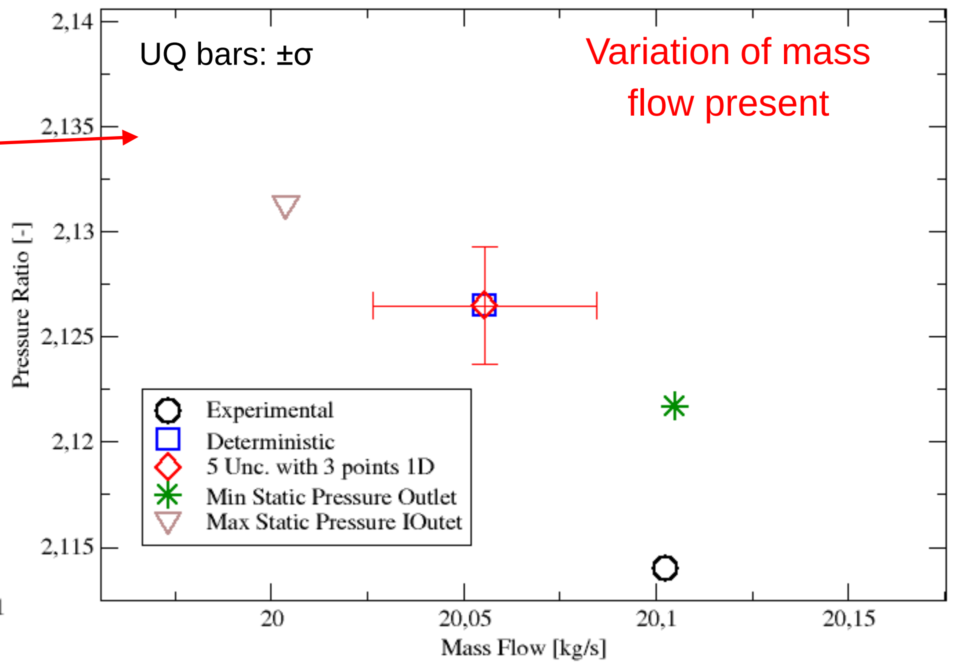

Application to Rotor 37

Non-deterministic analysis: Compressor map with only static outlet pressure as uncertain variable

- ❑ If only the static outlet pressure is chosen, the variation vanishes close to the choke mass flow

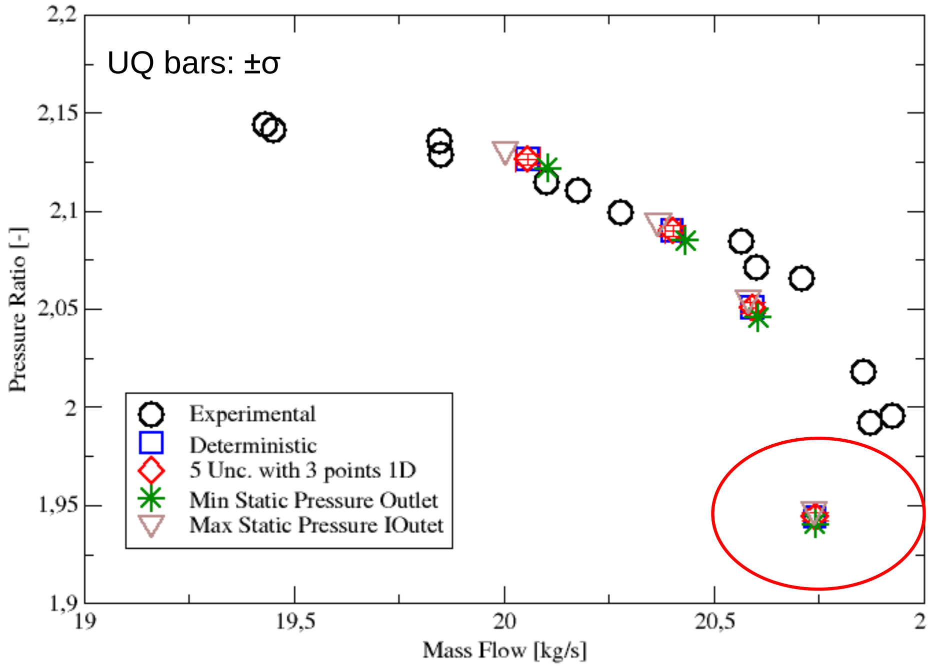

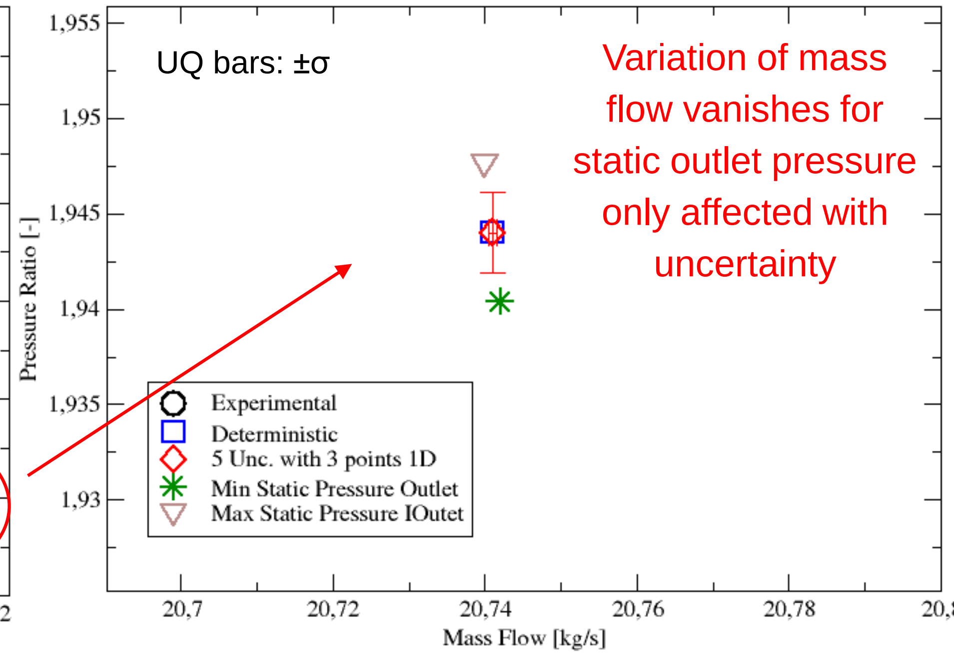

Compressor map with minimum/maximum value for total inlet pressure

- The compressor map for minimum/maximum value of the total inlet pressure is compared with the mean

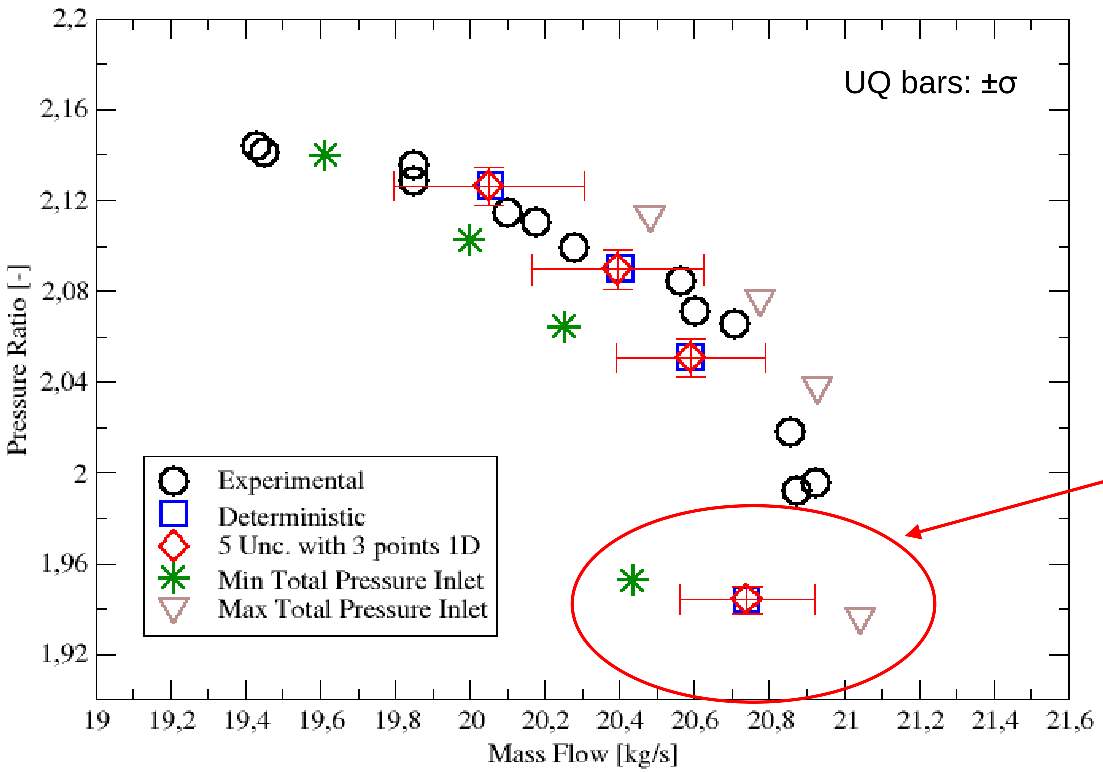

Variation of total inlet pressure modifies the choke mass flow

Min/Max values for a selection of uncertainties

- How to systematically assess influence of any uncertainty on the non-deterministic output
- Scaled sensitivity derivatives

Leading edge angle

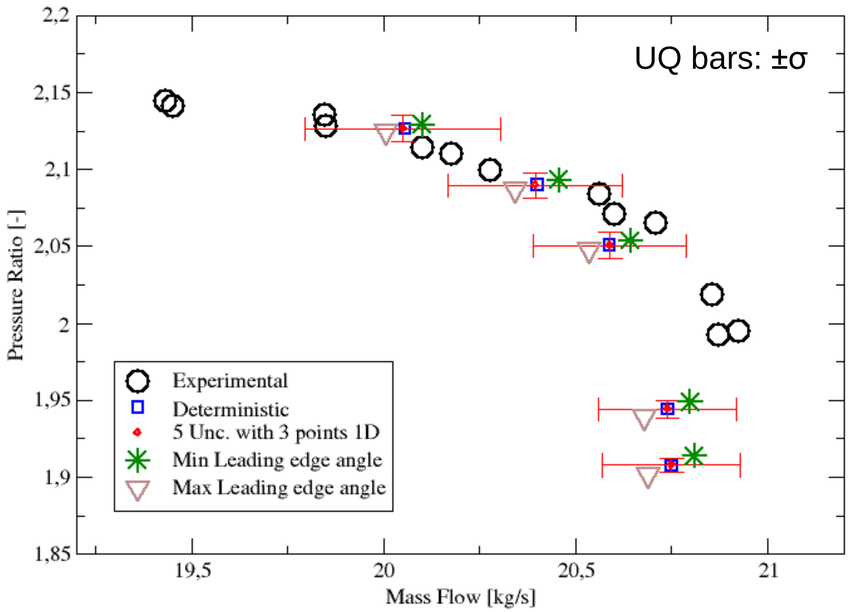

Trailing edge angle

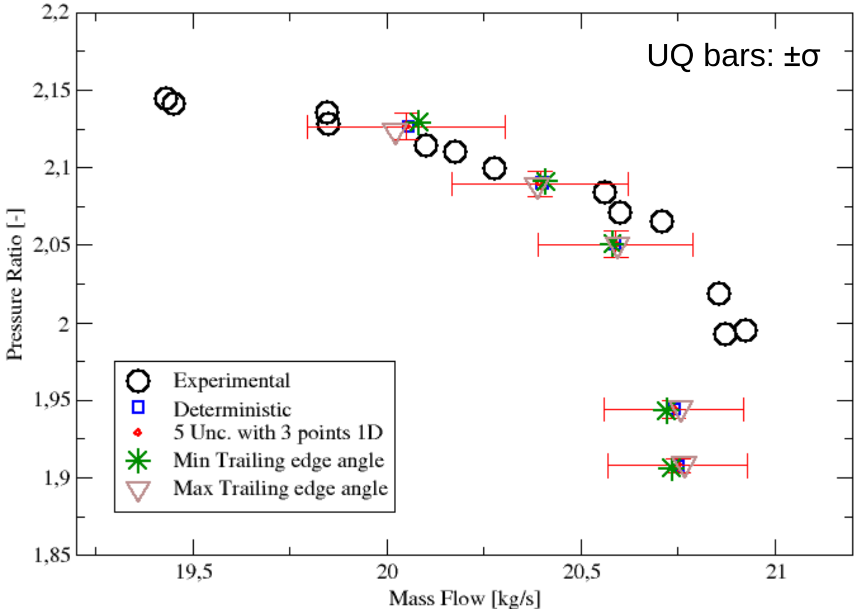

Application to Rotor 37

Scaled sensitivity derivatives

- Sensitivity derivatives allow to assess influence of a given uncertainty on the non-deterministic output systematically

$$s = \sigma_i \frac{\partial u}{\partial a_i}$$

- Total inlet pressure most dominant for pressure ratio and mass flow rate

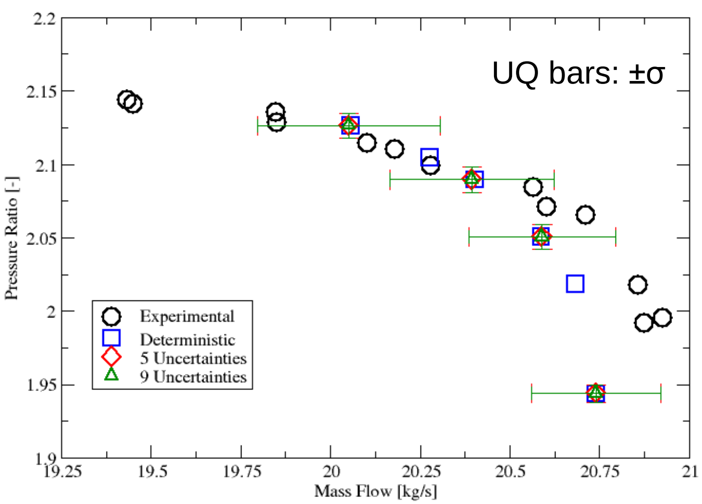

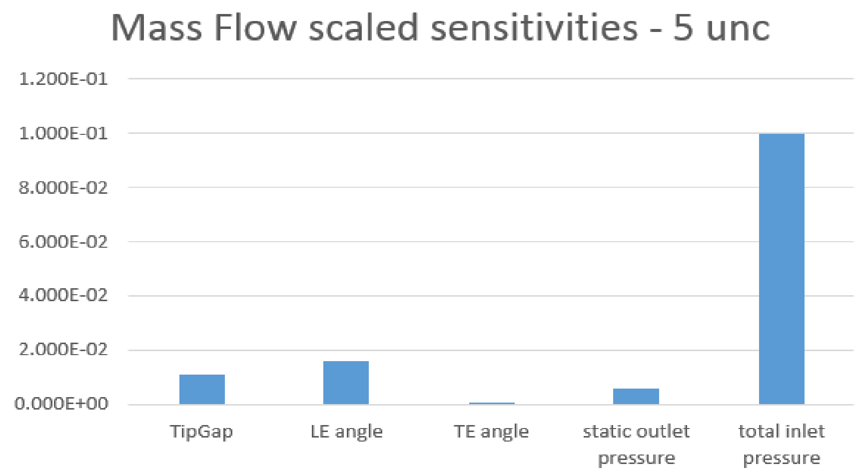

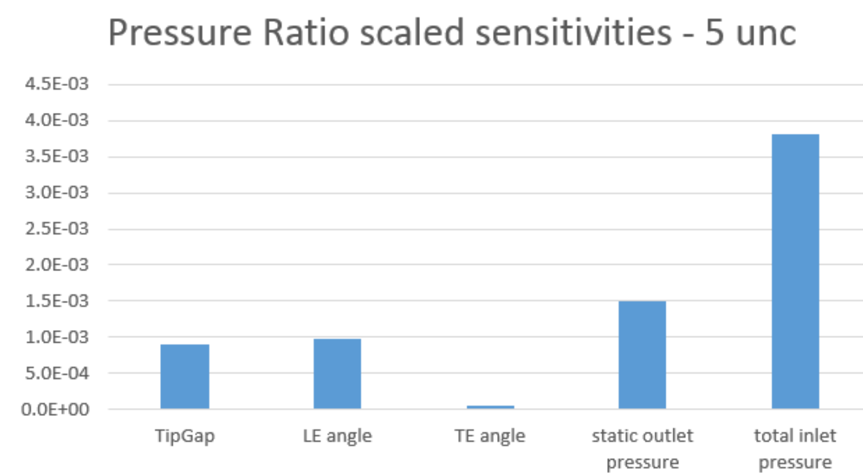

Application to Rotor 37

Scaled sensitivity derivatives

- Sensitivity derivatives allow to assess influence of a given uncertainty on the non-deterministic output systematically
- Most influential parameter for efficiency is the LE angle
- Dimension of scaled sensitivities is the as the quantity for which it is built

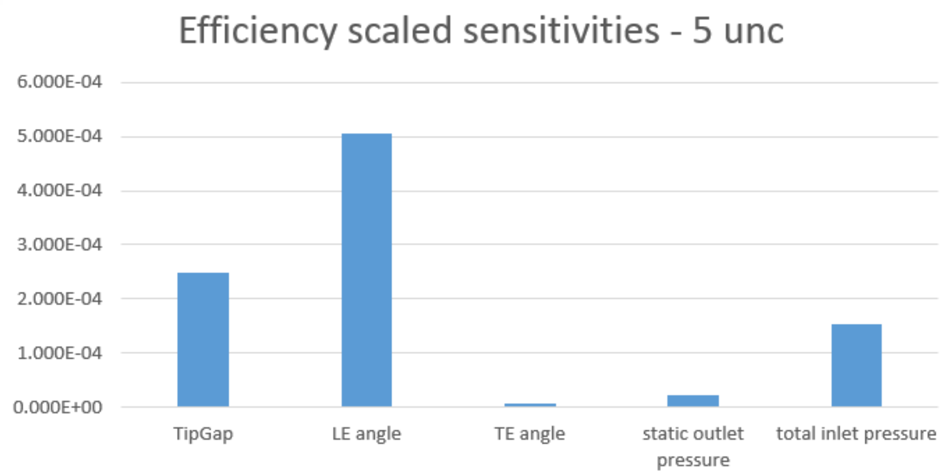

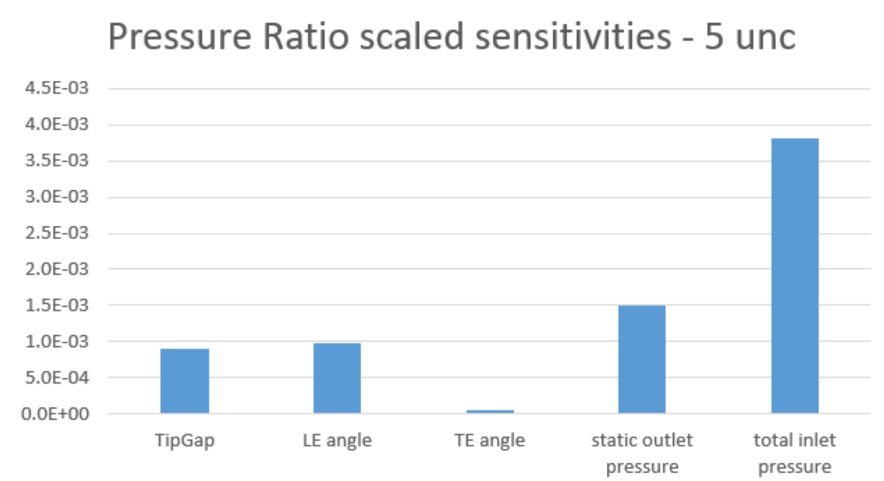

Application to Rotor 37

Non-deterministic analysis: Compressor map comparison coarse mesh

- Comparison of retained solution independent mesh with 4.7Mio cells and a coarser mesh with 700k cells
- Mean value of output PDF changes, but PDF shape is comparable (standard deviation)
- This indicates a relative independence of the UQ model from the mesh resolution
- This is also investigated by several groups working on reduction of uncertain space and sampling of covariance matrices needed for Karhunen-Loeve decomposition

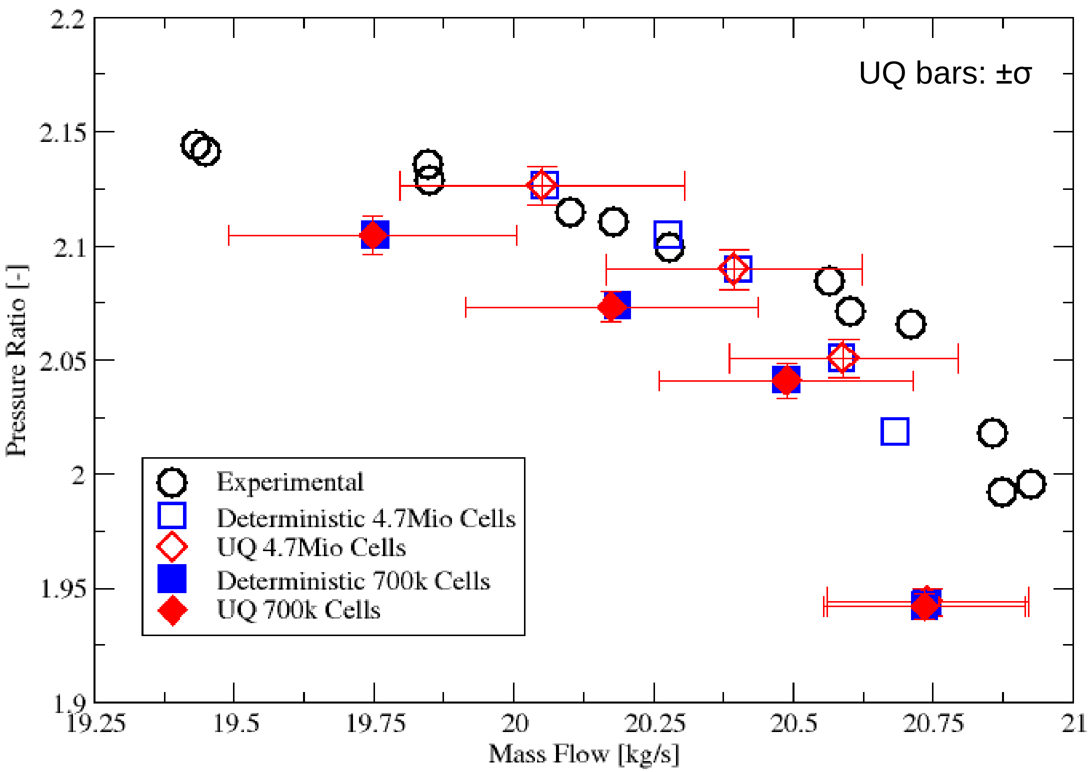

Test case description: RAE 2822

- Detailed description of geometry, exp. set-up and a series of simulations cross-plotting the predictions can be found in [5]

- Test case and UQ model
  - Mesh size: 165 638 cells
  - RANS + Spalart-Allmaras
  - 2D simulation
  - Use of CPU-Booster in FINE^{TM}/Turbo

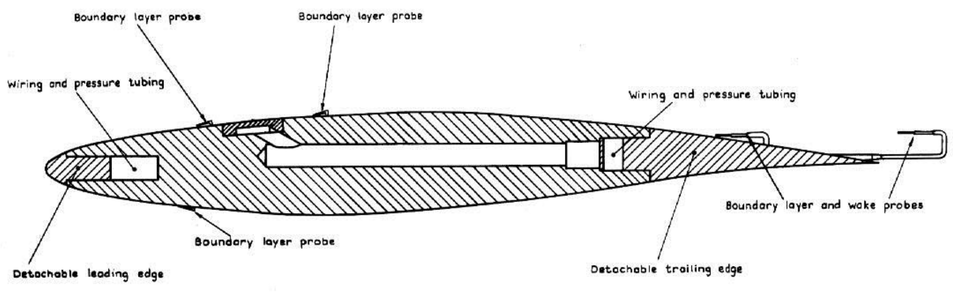

- Flow conditions
  - Case 9 in [AGARD-AR-138]
  - $M_{FreeStream} = 0.730$
  - $\alpha = 3.19°$
  - Re=6.5e6

Overview of imposed uncertainties

- Geometrical uncertainties

Parameter Name	PDF type	Most likely value	Minimal value	Maximal value
thickness-to-chord ratio	Beta	nominal	97 % * nominal	103% * nominal
Control points for thickness	Beta	nominal	97% * nominal	103% * nominal
Control points for camber curve	Beta	nominal	nominal - 0.01% chord	nominal + 0.01% chord

- 1 uncertainty
  - Thickness-to-chord ratio
- 4 uncertainties
  - Thickness law on 4 points
- 7 uncertainties
  - Camber curve on 6 points and thickness-to-chord ratio
- 10 uncertainties
  - Thickness law on 4 points and camber curve on 6 points

Application to RAE 2822

Automatic generation of meshes with varying thickness-to-chord ratio

- Same mesh size for <u>automatically</u> generated geometries with **varying thickness**

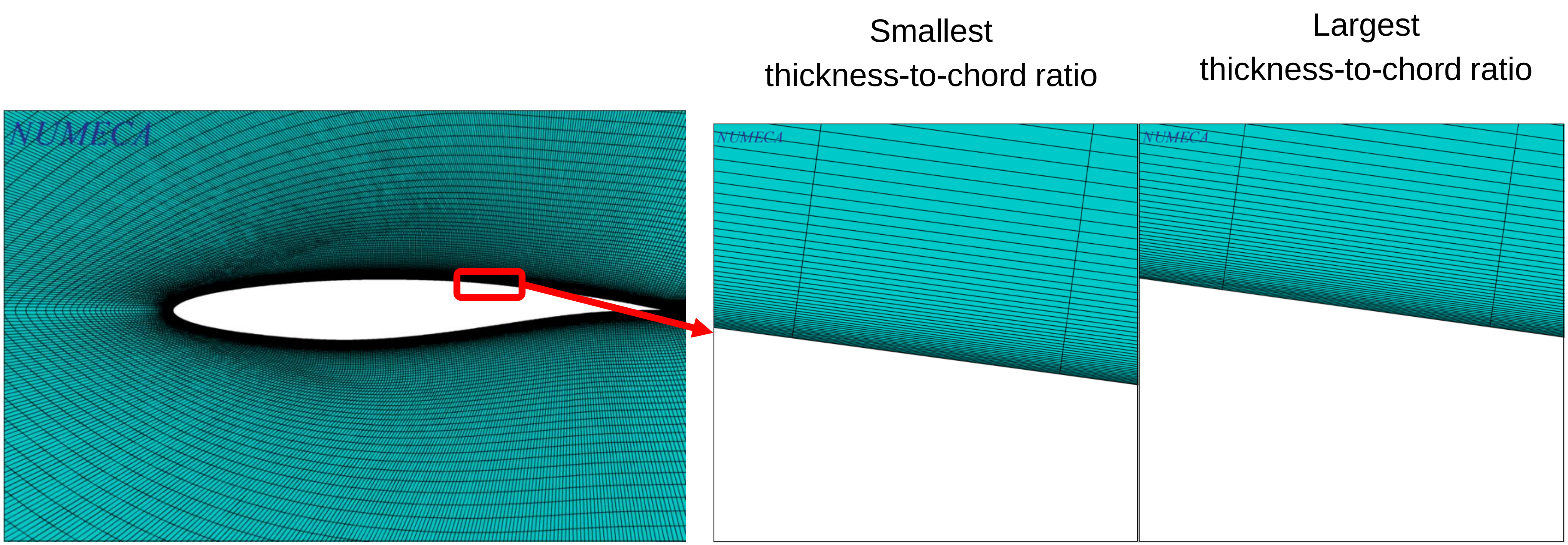

- Small variation on geometry

Application to RAE 2822

Automatic generation of meshes with varying camber line

- Scaled (increased modification) variation of **varying camber line**

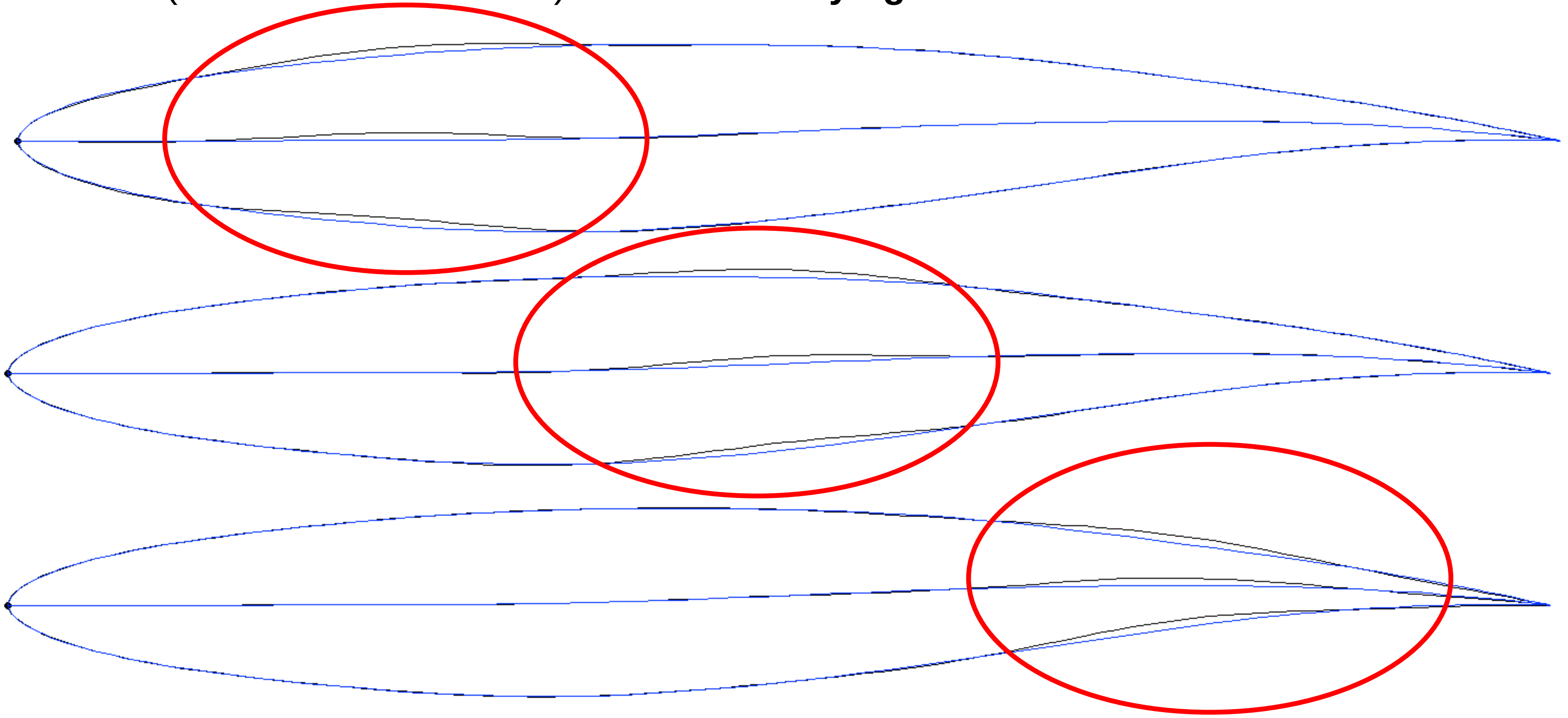

Automatic generation of meshes with varying camber line

- Same mesh size for <u>automatically</u> generated geometries with **varying camber line**

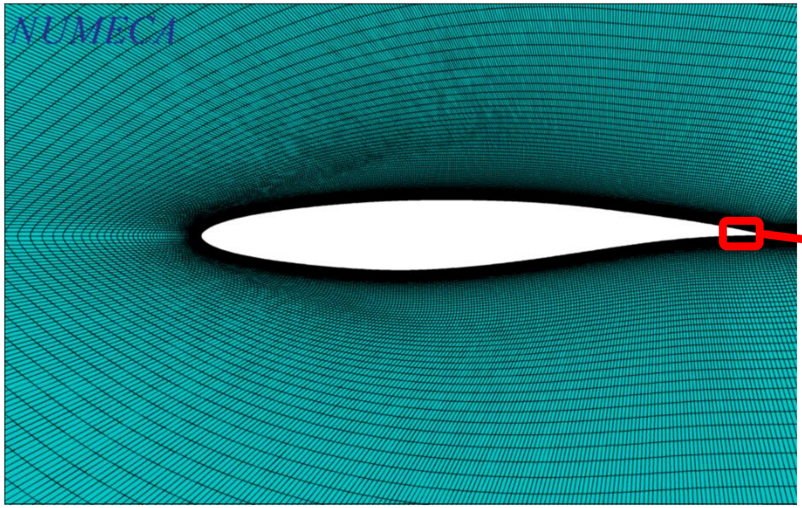

Smallest camber

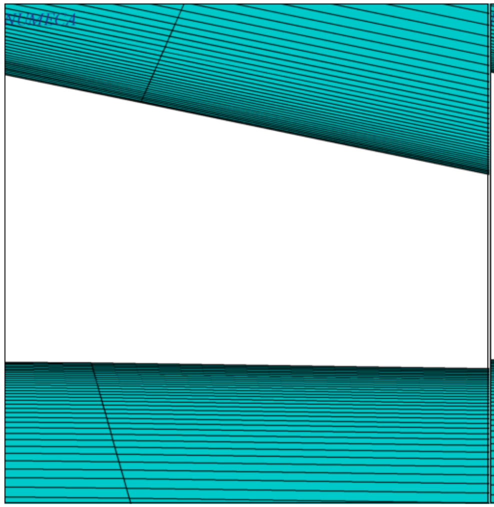

Largest camber

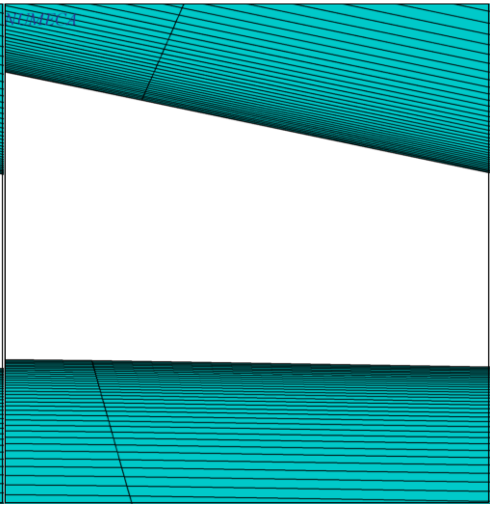

Non-deterministic analysis: overview

- ❑ Simulation characteristics
  - ❑ Mesh independent solution with 165 638 cells
  - ❑ RANS + Spalart-Allmaras
  - ❑ Use of CPU-Booster in FINE^{TM}/Turbo

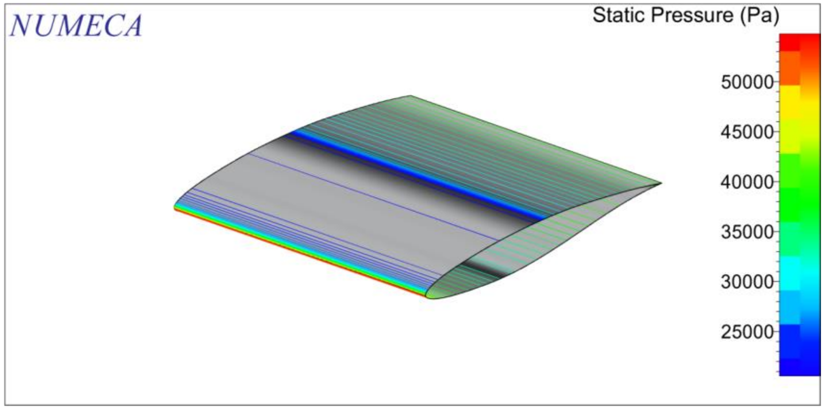

- ❑ UQ characteristics
  - ❑ 1 and 4, 7 and 10 uncertainties

Parameter Name	PDF type	Most likely value	Minimal value	Maximal value
thickness-to-chord ratio	Beta	nominal	97 % * nominal	103% * nominal
Control points for thickness	Beta	nominal	97% * nominal	103% * nominal
Control points for camber curve	Beta	nominal	nominal - 0.01% chord	nominal + 0.01% chord

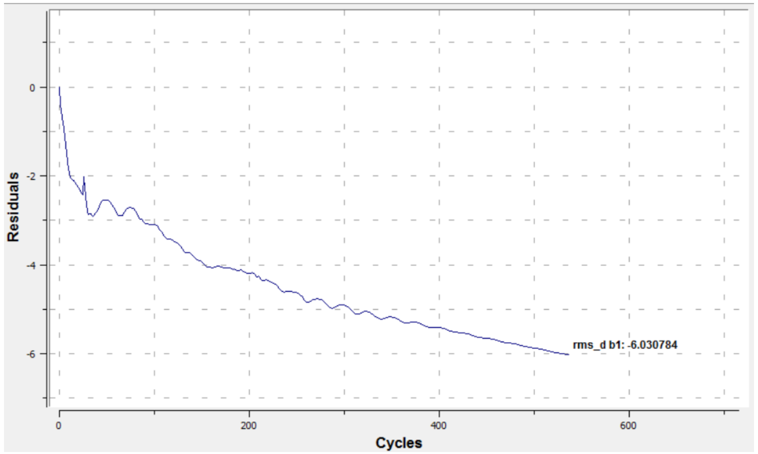

Non-deterministic analysis: Flow field big picture

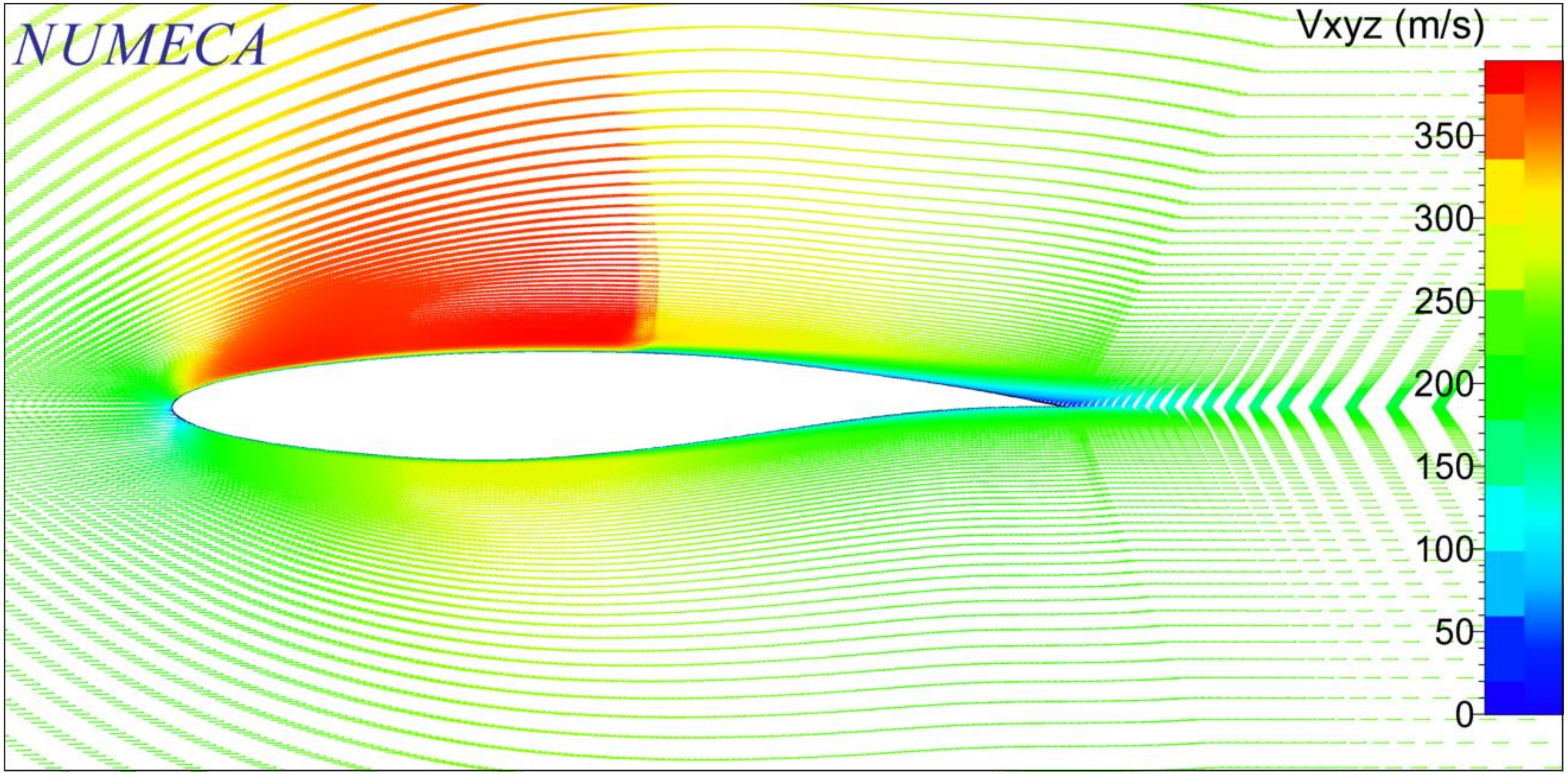

Application to RAE 2822

Non-deterministic analysis: C_p on blade surface - UQ

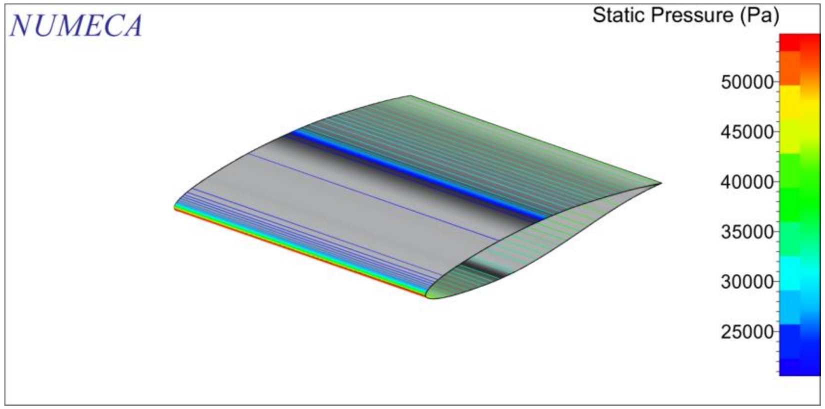

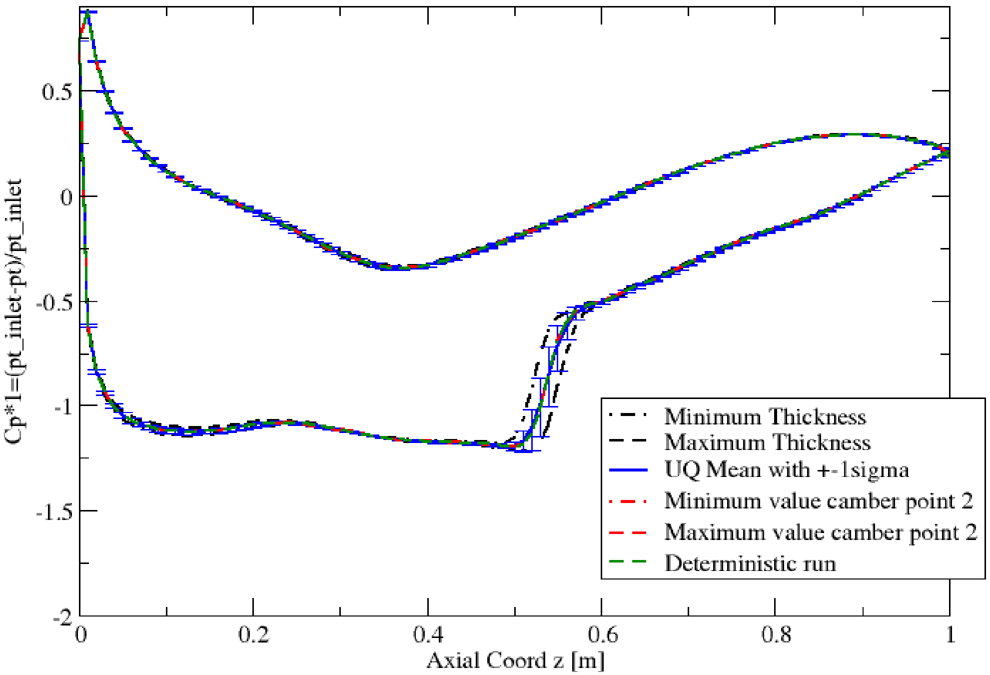

- Solution is now a PDF represented by its first two statistical moments
- Individual non-deterministic sub-computations provide some kind of sensitivity
- Uncertainty in solution is the largest in the near shock region

Application to RAE 2822

Non-deterministic analysis: C_p on blade surface – UQ and Sensitivity

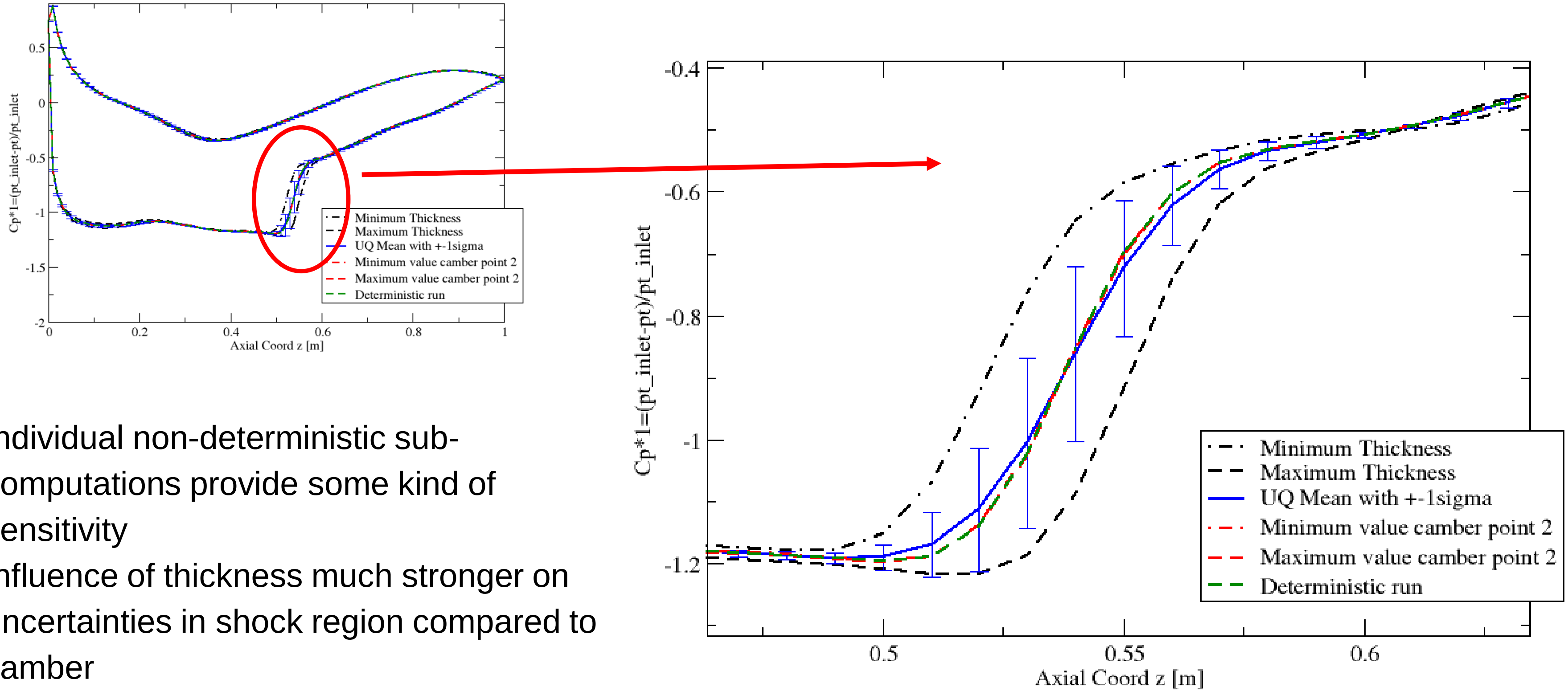

- Individual non-deterministic sub-computations provide some kind of sensitivity
- Influence of thickness much stronger on uncertainties in shock region compared to camber
- This kind of evaluation can be conducted for any flow phenomenon of interest

Application to Rotor 37

Non-deterministic analysis: C_p on blade surface – uncertainties models

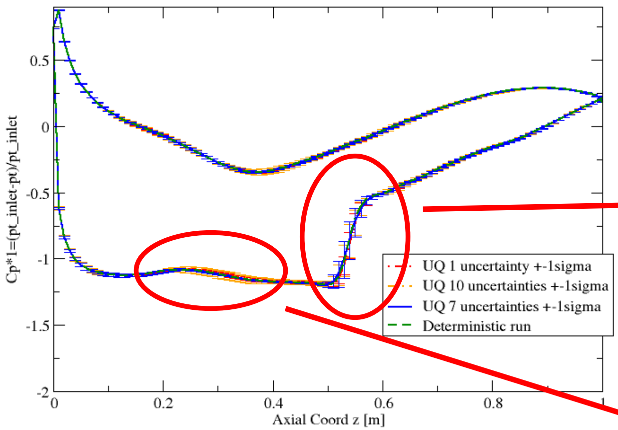

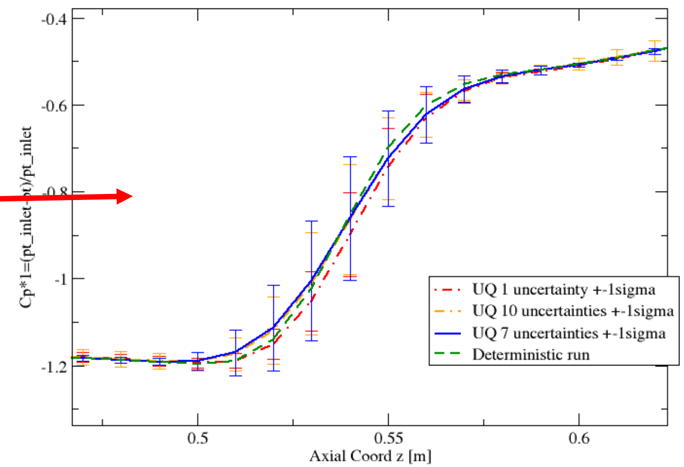

- Uncertainties for different uncertainty models
- Models of uncertainties have a small impact on mean and variance
- Modification of global thickness or local modification does not provide same mean and variance

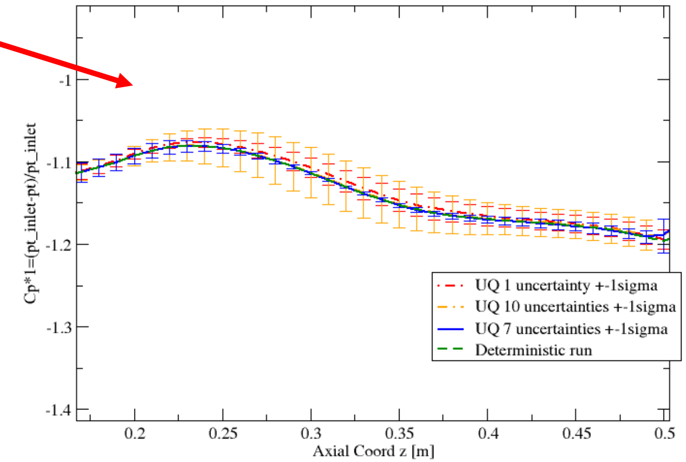

Application to RAE 2822

PDF reconstruction - verification

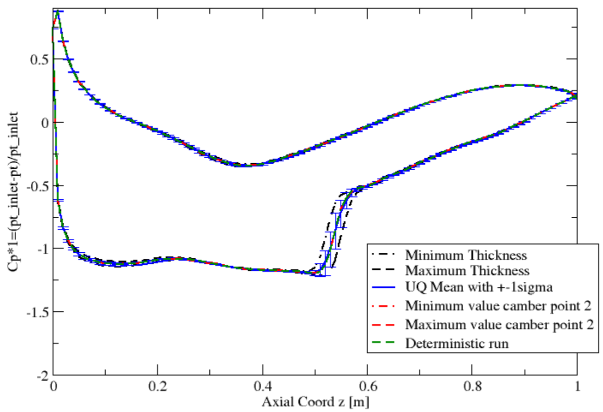

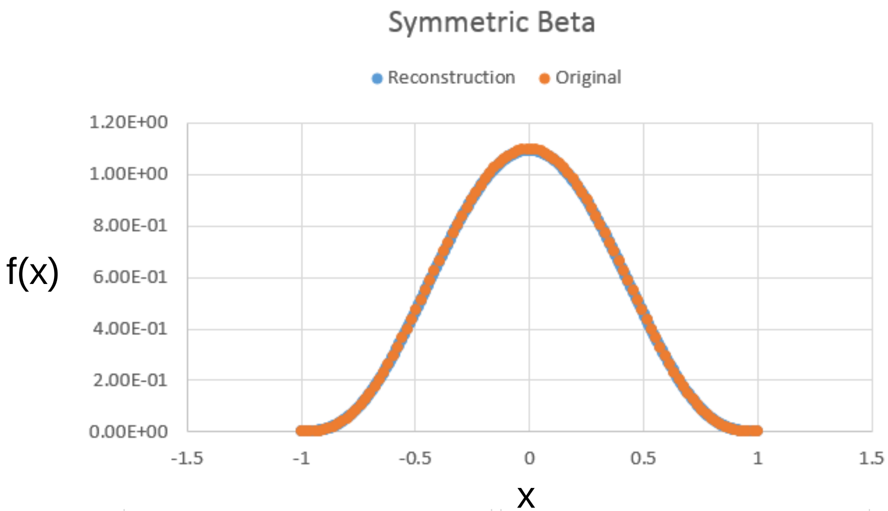

- ❑ Verification with known shapes of beta PDF
- ❑ Reconstruction with Pearson based on statistical moments of output PDF
- ❑ More information than centered UQ-bars around mean value, which implies symmetry due to lack of information of higher moments

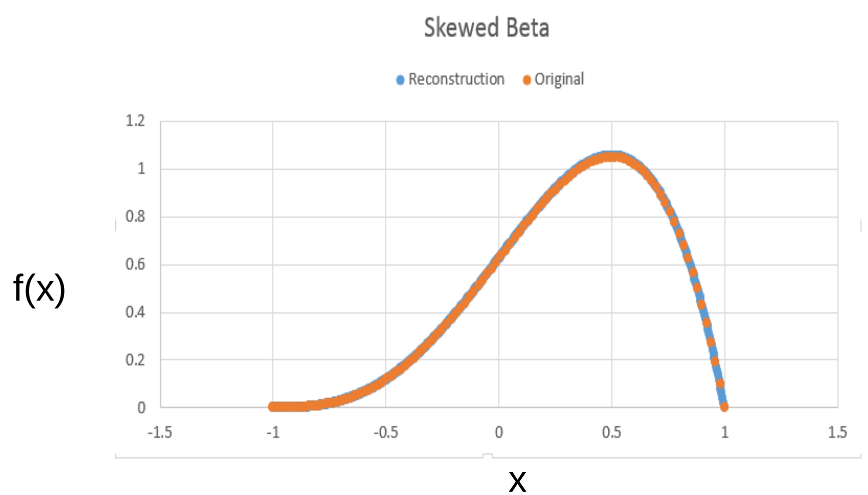

Application to RAE 2822

PDF reconstruction

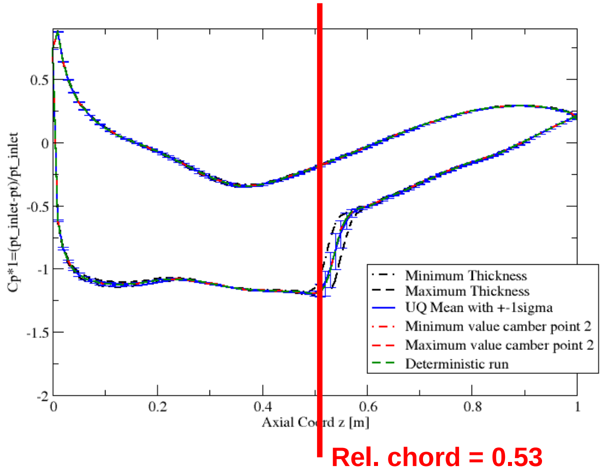

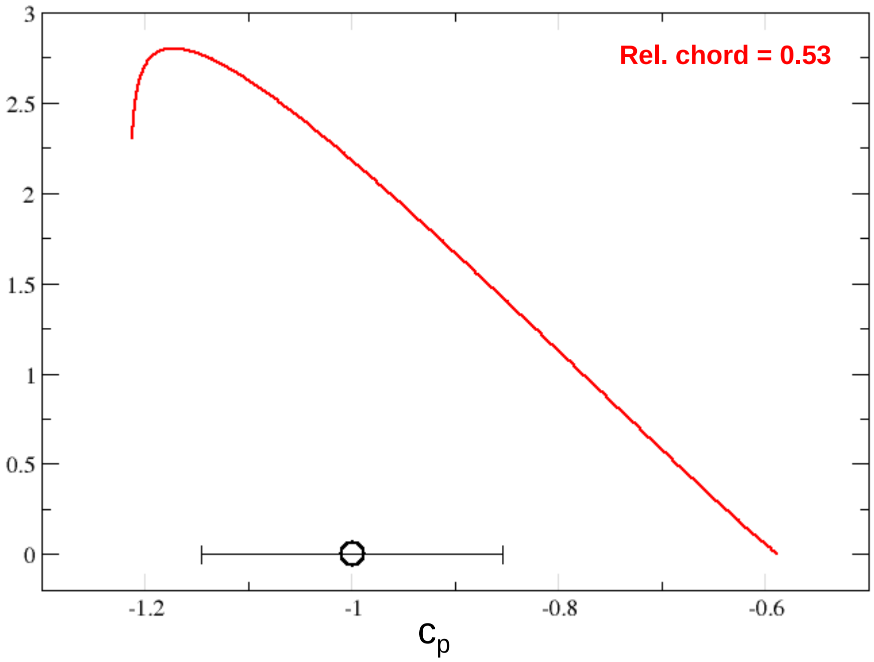

- Reconstruction at point relative chord 0.53
- Mean and UQ-bars indicate symmetric PDF
- Higher moments show a skew PDF

Outline

- ❑ Context
- ❑ UQ tool for simultaneous operational and geometrical uncertainties implemented in FINE^{TM}
- ❑ Application of Uncertainty Quantification in Industrial Applications
- ❑ **Perspective**

Where to go from here?

- ❑ Treatment of generalized geometrical uncertainties
    - ❑ Uncertain fields in addition to parameterized geometrical uncertainties
    - ❑ Uncertain profiles as boundary conditions vs. constant values
- ❑ Robust design – design under uncertainties
    - ❑ Account for uncertainties in the optimization process
    - ❑ Drastic increase in computations to be performed
        - ❑ Reduction of uncertain space is important
- ❑ Extend to arbitrary geometries
- ❑ Open to custom flow solvers and structural mechanics codes

References

Dunham J, 1998, *CFD validation for propulsion system components*, AGARD-AR-355

Golub GH, Welsch JH, 1969*, Calculation of Gaussian Quadrature rules*, Math. Comp. 23:221-230

Green L, (2011), *Lecture on Advanced Uncertainty Analysis*, NASA/NIA Summer Design Institute on Uncertainty, August 4, 2011

Loeven, GJA, 2010, *Efficient uncertainty quantification in computational fluid dynamics, Doctoral thesis*, Technische Universiteit Delft

Pearson K, 1895, 1901, 1915, Philosophical Transactions of the royal Society of London. 8 laws variant.

Roge G, 2013, *Foundations of Method of Moments - Lecture 1*, Mathematical Methods and Tools in Uncertainty Management & Quantification, Ercoftac course

Smolyak S, 1963, *Quadrature and Interpolation formulas for tensor products of certain classes of functions*, Dokl. Adad. Nauk USSR B, 240-243

Various, 1979, *EXPERIMENTAL DATA BASE FOR COMPUTER PROGRAM ASSESSMENT* - Report of the Fluid Dynamics Panel Working Group, AGARD-AR-138, ISBN 92-835-1323-1

Acknowledgement

"The research leading to these results has gratefully received funding from the European Union's Seventh Framework Programme (2007-2013) under grant agreement number 605036, UMRIDA project."